



## A first look at the N- and O-glycosylation landscape in anuran skin secretions



Eder Alves Barbosa <sup>a, b</sup>, Gabriel Sérgio Costa Alves <sup>c</sup>, Marcelo de Melo Andrade Coura <sup>d</sup>, Higor de Lima e Silva <sup>a</sup>, Filipe Souza da Rocha <sup>a</sup>, João Bueno Nunes <sup>a</sup>, Matheus de Souza Watanabe <sup>a</sup>, Alan Carvalho Andrade <sup>e, f</sup>, Guilherme Dotto Brand <sup>a, \*</sup>

<sup>a</sup> Laboratório de Síntese e Análise de Biomoléculas - LSAB, Instituto de Química - IQ, Universidade de Brasília – UnB, Brasília, DF, Brazil

<sup>b</sup> Laboratório de Espectrometria de Massa – LEM, Embrapa Recursos Genéticos e Biotecnologia, Brasília, DF, Brazil

<sup>c</sup> Laboratório de Processos Biológicos e Ativos Biotecnológicos – LPBAB, Instituto de Ciências Biológicas – IB, Universidade de Brasília – UnB, Brasília, DF, Brazil

<sup>d</sup> Divisão de Cirurgia Colorretal, Hospital Universitário de Brasília, Escola de Medicina, Universidade de Brasília – UnB, Brasília, DF, Brazil

<sup>e</sup> Universidade Federal de Lavras, Campus UFLA, Lavras, MG, 37200-000, Brazil

<sup>f</sup> Embrapa Café, INOVACAFÉ, Campus UFLA, Lavras, MG, 37200-000, Brazil

### ARTICLE INFO

#### Article history:

Received 17 August 2021

Received in revised form

8 January 2022

Accepted 17 January 2022

Available online 22 January 2022

#### Keywords:

Mass spectrometry

Glycomics

Transcriptomic

Oligosaccharides

Amphibian's skin secretion

### ABSTRACT

Amphibians secrete a complex array of molecules that shape their interactions with coinhabiting microorganisms and macroscopic predators. Glycans are a rapidly evolving and complex class of biomolecules implicated in intrinsic and extrinsic recognition events. Despite the numerous studies aiming at the biochemical characterization of anuran skin secretions, little is known about protein-linked oligosaccharides, their synthesis pathways, and their homing secreted glycoproteins. In the present report, LC-MS/MS was used to investigate the diversity of N- and O-linked oligosaccharides in the skin secretion of two South American frogs, *Pithecopus azureus* and *Boana raniceps*. Additionally, the enzymes responsible for glycan synthesis pathways were evaluated based on their skin tissue transcriptome. Our analyses allowed the annotation of various N- and O-glycan structures commonly found in vertebrate proteins. Paucimannosidic glycans were abundant in the skin secretion of both amphibians; however, hybrid and complex N-glycan structures were detected only in *B. raniceps*. A good correlation between the structures discovered in glycomics analyses and transcripts encoding enzymes necessary for their synthesis was obtained. Some transcripts such as those of MAN1A2, FUT8, and ST6GALNAC were found solely in *B. raniceps*. Finally, secreted N- and O-linked glycoproteins were predicted from the transcriptomic data, indicating that proteases and protease inhibitors are putative sources of the glycans described herein. Overall, our results show the presence of oligosaccharides in amphibians skin secretions and suggest that their diversity is species-specific, paving the way for novel perspectives involving amphibian evolution and ecology.

© 2022 Elsevier B.V. and Société Française de Biochimie et Biologie Moléculaire (SFBBM). All rights reserved.

### 1. Introduction

The pioneering studies of Dr. Vittorio Ersparmer provided invaluable information on the skin secretions of amphibians, which rendered these a prominent position among vertebrates as sources

of pharmacologically active molecules [1,2]. Since these early days, ongoing efforts in the biochemical and biophysical characterization of frog skin secretions resulted in expanding collections of bioactive amines, alkaloids, steroids, peptides, and proteins with myriad biological activities [3,4]. At first thought to have endogenous physiological regulatory roles [5], the occurrence of these secreted molecules in the amphibian integument was increasingly associated with the ecological relations they hold with their environment and with other organisms [2]. The current paradigm states that some of these molecules constitute chemical tools that help to

\* Corresponding author. Laboratório de Síntese e Análise de Biomoléculas – LSAB, Instituto de Química – IQ, Universidade de Brasília – UnB, Campus Universitário Darcy Ribeiro, CEP, 70910-900, Brasília, DF, Brazil.

E-mail address: [gbrand@unb.br](mailto:gbrand@unb.br) (G.D. Brand).

shape their interaction with macroscopic organisms, e.g., predators, and with the ever-present microscopic commensal and pathogenic microbiota, conferring selective advantage over amphibians with impaired antimicrobial defenses.

Despite the growing knowledge on the chemical composition of frog skin secretions accumulated throughout the years, little is known about the protein-linked glycans that decorate secreted glycoconjugates and the vast number of glycosyltransferases and glycosidases that catalyze their synthesis. Indeed, studies on the diversity of glycan species in amphibians are mostly related to O-linked glycans from egg jelly proteins, which are thought to modulate the specificity of gamete recognition and parasitism [6–8]. These are primarily derived from mucin-type glycoproteins that are synthesized by specific regions in the oviduct [9]. Also, a mucin from the mucus barrier of *Xenopus laevis* tadpoles has been described [10]. The characterization of protein-linked glycans in skin secretion of adult specimens constitutes relevant knowledge in evolutionary and ecological perspectives, with still other implications in biochemistry and immunology. N- and O-glycosylation pathways have been studied in Archaea, Bacteria and Eukarya [11–13]. Among the latter, characteristic N-glycosylation patterns have been described for plants, yeasts, slime molds, insects, and vertebrates [12,14]. Amphibians are thought to be the first truly terrestrial vertebrates, undergoing the transition between the aquatic and terrestrial environments, and little is known about the diversity of glycans secreted as conjugates in their skin and the impact this transition may have imparted in this class of molecules. From an ecological point of view, protein-linked glycans are of utmost relevance to intrinsic (e.g. cell-cell recognition) and extrinsic recognition events, like host-pathogen interactions [12]. Given the continuous contact amphibians have with water ponds, soil, and plant litter, their skin is populated by a diverse array of microorganisms, like bacteria, archaea, fungi, viruses and protozoans [15]. Nevertheless, multiple studies have demonstrated that the resident microbiota differs significantly from the environment, indicating that the amphibian skin is a selective microbial niche [16,17], where commensal bacteria may display still other putative roles, such as hindering the colonization of opportunistic microorganisms [18]. Similarly to the human gut [19], glycans in amphibian skin are thought to contribute in the discrimination of symbiotic/commensal microbes and pathogens, comprising, along with other molecules (e.g. antimicrobial peptides), and mechanisms (e.g. skin sloughing [20]), a system for the control of the commensal microbiota [21]. However, little is known about the N- and O- glycans secreted by amphibians in the form of glycoconjugates.

The present study aims to investigate the diversity of N- and O-linked glycans in the skin secretions of *Pithecopus azureus* and *Boana raniceps*, two anurans from the Brazilian fauna, using a mass spectrometry-based glycomics approach. In addition, it intends to identify the enzymes involved in N- and O-glycan biosynthesis pathways by analyzing anuran skin transcriptomes. Moreover, secreted glycoproteins are predicted, thus identifying the putative protein sources of these glycans. It is our understanding that the present study yields knowledge about a poorly studied class of biological molecules in amphibian skin secretions, N- and O-glycans, and considers their putative relevance to the biology of amphibians.

## 2. Material and methods

### 2.1. Biological samples

*Pithecopus azureus* and *Boana raniceps* were manually captured in Niquelândia and Flores - Goiás, respectively. All procedures

involving animals were authorized by competent organs: Instituto Chico Mendes de Conservação da Biodiversidade (17851–1 and 31066–1) and legal Ethics Committee on Animal Use (UnBDOC n° 29077/2009 and 119267/2011). The crude extracts from amphibians were obtained by electric stimulation, (two stimuli of 30 s each). Frogs were washed with cold Milli-Q water and secretions were collected in tubes of 50 mL kept on ice. Samples were immediately frozen and lyophilized.

### 2.2. Isolation of N-linked oligosaccharides

The freeze dried skin secretions of *P. azureus* and *B. raniceps* were submitted to N-glycan extraction procedures using a previously described methodology [22]. Briefly, 10 mg of the dry skin secretions were dissolved in 240 µL of 0.6 M Tris containing 6 M guanidine chloride and left under agitation for 90 min at 45 °C. Then, proteins were reduced by adding 44 µM DTT (final concentration) and incubating the samples for 4 h at 45 °C. Protein alkylation was then performed at room temperature, in the dark, for 17 h, using 131 mM iodoacetamide. Alkylated protein samples were later transferred to size-exclusion Centricon filters with 10-kDa cut-off and added with 200 µL of 50 mM ammonium carbonate solution, followed by centrifugation for 14 min at 14,000 rpm. The buffer exchange procedure using ammonium carbonate and centrifugation was repeated three times, resulting in a final volume of approximately 22 µL. Then, 214 µL of 50 mM ammonium carbonate containing 14 µg trypsin were added to samples, which were incubated under agitation (400 rpm) for 24 h at 37 °C. After protein digestion, enzymes were inactivated by heat (10 min at 100 °C) and samples were freeze dried. These were later dissolved in 200 µL of 50 mM carbonate containing 15 mU of PNGase F, incubated at 37 °C for 15 h and freeze-dried. Samples were dissolved with 200 µL of 5% (v/v) acetic acid and purified using Sep-Pak C18 cartridges. Free N-glycans were eluted from cartridges using 3 mL of 5% acetic acid, and subsequently freeze dried and stored at -20 °C until further use.

### 2.3. Isolation of O-linked oligosaccharides

O-glycans were isolated as previously described [22]. Briefly, 10 mg of the dried skin secretion of both frogs were individually dissolved with 200 µL of a fresh solution constituted of 4 M NaBH<sub>4</sub> and 200 mM NaOH. This constitutes a β-elimination procedure, which was performed without prior N-glycan release. Samples were incubated at 45 °C for 8 h and the reactions were stopped by adding acetic acid. Released O-linked oligosaccharides were purified using a Dowex resin (50 × 8, H<sup>+</sup>, 50–100) packed in a Pasteur pipet, eluting with 4 mL of 5% acetic acid. Samples were freeze dried and the borate salts were removed by repeated addition of 500 µL methanol with 5% acetic acid and evaporation using a stream of argon gas, a procedure that was repeated five times. Samples were freeze dried and stored at -20 °C until further use.

### 2.4. Permethylation of N- and O-linked oligosaccharides

Freeze dried samples were dissolved in 500 µL DMSO saturated with 25 mg of freshly added NaOH. Aliquots (300) µL of iodomethane were added to the solution followed by atmosphere replacement using argon and sonication for 90 min. The permethylation reaction was stopped by adding 1 mL of 5% acid acetic in an ice bath. Permethyated N-glycans were extracted using 600 µL of chloroform twice, washed nine times with water, and dried under a stream of argon. For their purification, samples were dissolved in methanol, applied to a Sep-Pak C18 column (previously equilibrated with water) and washed with 10% (v/v) acetonitrile.

Permethylated N-glycans and O-glycans were eluted with 80% acetonitrile, and then collected and freeze dried.

## 2.5. Mass spectrometry acquisition and analysis (LC-MS)

Dried samples were dissolved in 40  $\mu$ L methanol containing 10 mM sodium acetate. Analyses were performed by injecting 6  $\mu$ L of each sample in an Eksport ultraLC 100 (Sciex, Framingham, MS, USA), equipped with a Kinetex (2.6  $\mu$ , C18, 100 Å, 50  $\times$  2.1 mm) column, coupled to a TripleTOF 5600+ mass spectrometer. Chromatography was performed at a flow rate of 0.4 mL/min. Column was kept at 40 °C. Mass spectrometer operated in the positive and high-resolution mode. The mass ranges of acquisitions were at  $m/z$  800–2000 for N-glycans and  $m/z$  200–2000 for O-glycans. Other acquiring parameters were: curtain gas = 15; number of cycles = 217; polarity = positive; period cycle time = 525 ms; pulser frequency = 13.569 kHz and accumulation time = 500.00 ms. Mass spectrometer was calibrated using APCI positive calibration solution before acquisitions. MS/MS spectra were obtained using the Information Dependent Acquisition (IDA) mode. Ions from charge state 1 to 4 were selected for fragmentation using dynamic collision energy mode.

MS data were converted to mzXML format using MSConvert (ProteoWizard 3.0). Fragmentation spectra (MS/MS) were automatically annotated using GRITS Toolbox 1.2 software according to the following parameters: 5.0 ppm of accuracy MS; 50 ppm of accuracy MSn; 5.0% of fragment intensity cut-off; perMe derivatization type; free reducing end for N-glycans and reduced end for O-glycans; maximum of 3 cleavages; maximum of 1 cross ring cleavages; glycosidic cleavages of B, Y, C and Z series; cross ring cleavages of A and X series; maximum of 4 charges as Sodium adducts. GRITS was programmed to annotate either N- or O-glycan ions from their corresponding LC-MS/MS data. The annotated spectra were revised using GlycoWorkbench 2.1 build 146 software. Additionally, some spectra whose precursor ion mass matched accurately to N-glycans that were not annotated by GRITS Toolbox were analyzed and annotated using GlycoWorkbench software. Data in this publication was produced and reported in accordance with the guidelines laid out by the MIRAGE (minimal information required for a glycomics experiment) initiative [23]. Raw data and annotations were submitted to GlycoPost database (ID GPST000217) [24]. The symbol nomenclature for glycans was used in their representation throughout the manuscript [25].

## 2.6. RNA extraction and RNA-seq library preparation

Specimens of *P. azureus* and *B. raniceps* ( $n = 8$  for each species) were euthanized by intracranial injection of lidocaine [26]. The skin tissues were dissected and immediately frozen using liquid N<sub>2</sub>. Total RNA was extracted using Trizol reagent (Invitrogen) and treated with DNase-I. The integrity analysis and quantification of total RNA were performed in a Bioanalyzer (2100, RNA Nano 6000 Agilent). The 1st strand cDNA synthesis was performed using 1  $\mu$ g total RNA and the SMARTer™ PCR cDNA Synthesis Kit (Clontech). After double-stranded DNA synthesis, the DNA (~5  $\mu$ g) was nebulized to a mean fragment size of 650 bp, ligated to an adapter using standard procedures and then sequenced using GS-FLX Titanium (Beckman Coulter Genomics SA, Grenoble, France). All sequencing procedures (excepted RNA extraction) were performed by 454 Life Science/Roche Company (EUA).

## 2.7. Processing of RNA-seq reads

454 raw data were pre-processed using the mirabait to remove contaminants (non-coding RNA) and adapter. Assembly of the

reading sequences were performed with the MIRA software v. 3.4.1.1 [27] with the predefined parameters recommended for EST data obtained for Roche 454 equipment (-job = est, again, accurate, 454). The option (-GE: not = 10) was used to specify the number of threads that should be used for steps that can use multiple cores. The minimum score for alignment was set at 75 (-AL: mrs = 75) and the minimum size of the reading sequences at 100 base pairs (-AS: mrl = 100). Blast searches were performed online using standard algorithm parameters of Standard Nucleotide BLAST (BLASTN) from <https://blast.ncbi.nlm.nih.gov>.

## 2.8. Prediction of N-linked and O-linked glycosylation profile for the skin transcriptome

All glycosylation predictions were conducted over the potentially secreted batch of proteins sequences. Putative secreted protein was predicted using the SignalP 4.1 Server [28] (<http://www.cbs.dtu.dk/services/SignalP4.1/>). N-glycosylated proteins from *P. azureus* and *B. raniceps* skin secretions were predicted using the NetNGlyc 1.0 server (<http://www.cbs.dtu.dk/services/NetNGlyc/>), which is based in artificial neural networks that examine the sequence context of Asn-Xaa-Ser/Thr sequons. Sequences having N-glycosylation potential >0.75 were considered as cut-off value [29]. The identified predicted N-glycosylated proteins are listed in the Supplementary Materials 5 and 7. The NetOGlyc 3.1 server ([www.cbs.dtu.dk/services/NetOGlyc/](http://www.cbs.dtu.dk/services/NetOGlyc/)) was used to identify the O-glycosylation sequons from *P. azureus* and *B. raniceps* skin secretions, upon a neural network-based prediction of mucin type GalNAc O-glycosylation sites. The G-score is the score from the best general predictor; the I-score is the score from the best isolated site predictor. Gscore greater than 0.5 indicates a residue predicted as glycosylated, the reliability of the prediction being proportional to the score. For threonine amino acid residues, an additional score is used [30]. The identified predicted O-glycosylated proteins are listed in the Supplementary Materials 6 and 8. PANTHER Classification System [31] was used to analyze predicted N- and O-linked glycoproteins from both amphibians according to molecular function using sequence IDs.

## 3. Results

### 3.1. N-linked oligosaccharides from *P. azureus* and *B. raniceps* skin secretions

Proteins from the skin secretions of *P. azureus* and *B. raniceps* were subjected to reduction and alkylation, followed by trypsin hydrolysis and the PNGase F-mediated release of protein N-linked glycans. The free N-glycans resulting from these procedures were derivatized using iodomethane and purified by SPE. Samples were later submitted to LC-MS/MS analyses using a reverse phase C<sub>18</sub> column coupled to a mass spectrometer operating in positive mode. Mainly singly ([M + Na]<sup>+</sup>), doubly ([M + 2Na]<sup>2+</sup>) and triply ([M + 3Na]<sup>3+</sup>) charged sodium adduct ions were identified in the MS spectra of samples, and these were fragmented for putative structural annotation. Following the automated interpretation and manual inspection of MS and MS/MS spectra, seven ions compatible with N-linked oligosaccharides were identified in the skin secretion of *P. azureus*, whereas thirteen ions were identified in *B. raniceps*. These ions presented lower than 5 ppm mass error in relation to the theoretical masses of their corresponding N-glycans, and their fragmentation spectra were compatible with the proposed structures. To illustrate the glycan annotation pipeline adopted in the present study, the extracted ion chromatograms (XICs), and the MS and MS/MS spectra of HexNAc<sub>2</sub>Hex<sub>3</sub> (precursor ion [M + Na]<sup>+</sup> = 1171.5857 Da), and HexNAc<sub>2</sub>Hex<sub>2</sub>Fuc<sub>1</sub> (precursor

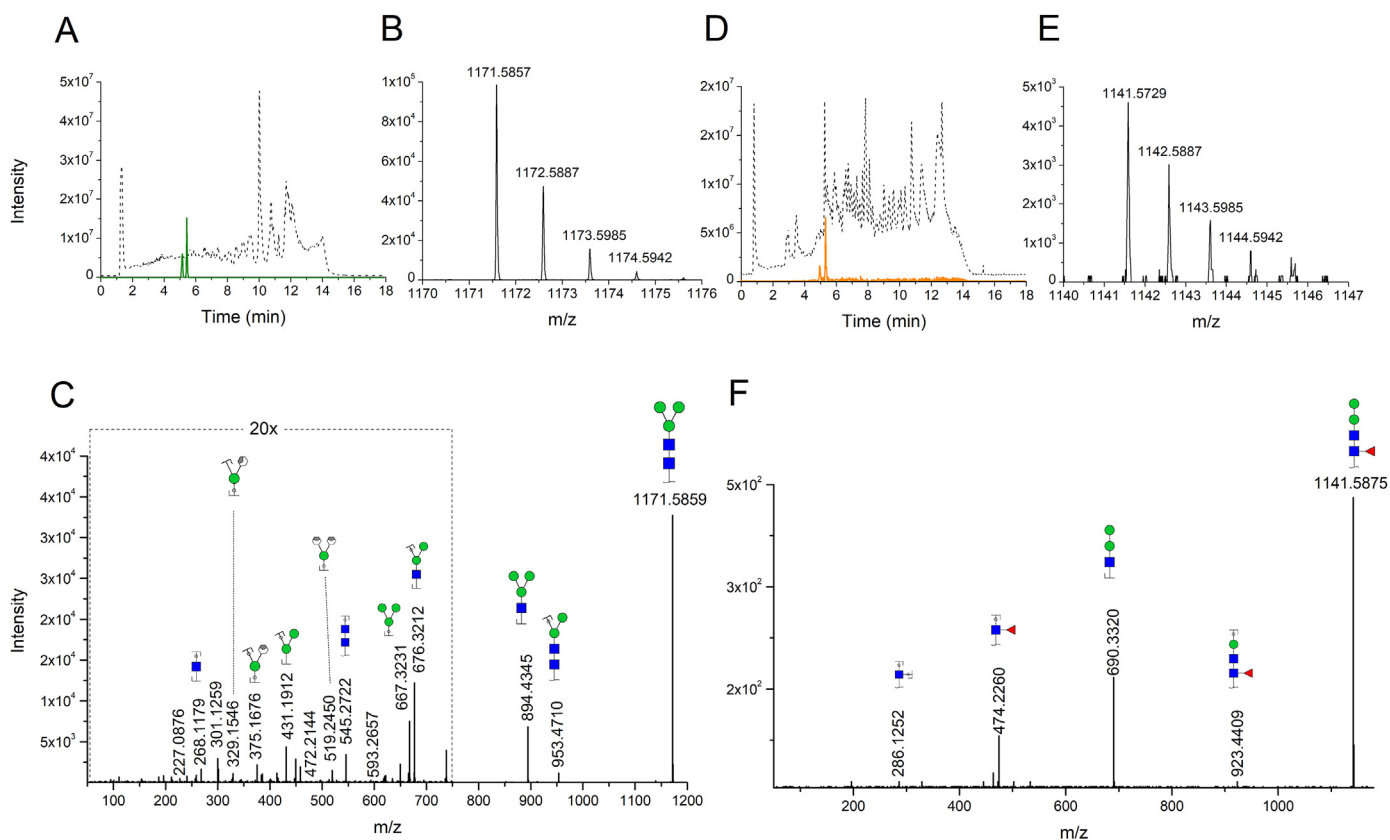
ion  $[M + Na]^+ = 1141.5729$  Da), are provided in Fig. 1A–F. Neutral losses of Hex and HexNAc residues were observed in the MS/MS spectrum of  $[M + Na]^+ = 1171.5857$  Da (Fig. 1C), and a characteristic ion,  $m/z$  474.2268, typical of core-fucosylated structures, was found in the fragmentation spectrum of  $[M + Na]^+ = 1141.5729$  Da (Fig. 1F). While HexNAc<sub>2</sub>Hex<sub>2</sub>Fuc<sub>1</sub> was putatively identified as F(6)M<sub>2</sub>, a core-fucosylated paucimannosidic glycan, the fragmentation spectrum of HexNAc<sub>2</sub>Hex<sub>3</sub> indicated the paucimannosidic glycan M<sub>3</sub>. The MS/MS spectra of all the N-glycans identified herein are provided as Supplementary Material 1. The putative N-glycan structures obtained from the skin secretion of *P. azureus* and *B. raniceps*, their theoretical and experimental masses, and their charge states, are listed in Table 1.

Extracted ion chromatograms were obtained for the N-glycans putatively identified in the skin secretion of *P. azureus* (Fig. 2A) and *B. raniceps* (Fig. 2B). More than one retention time was frequently observed for individual ions along the chromatographic run, as expected for non-reduced permethylated N-glycans due to the  $\alpha$ - and  $\beta$ -anomers generated after PNGase-F mediated hydrolytic release, as previously reported [32]. Qualitative and quantitative differences in the composition of samples were also made apparent. N-glycans in the *P. azureus* skin secretion were either paucimannosidic, such as M<sub>1</sub>, M<sub>2</sub>, and M<sub>3</sub>, or oligomannosidic, ranging from five to seven mannose residues attached to the chitobiose core (Fig. 2A). In addition, M<sub>4</sub>, was also detected. M<sub>3</sub> was the most abundant N-glycan in the *P. azureus* extract, with a peak area equivalent to  $45 \pm 18\%$  of all the oligosaccharide compositions

(Supplementary Table 1). On the other hand, *B. raniceps* showed a greater diversity of N-glycan structures in its skin extract, including paucimannosidic, mannose-rich, hybrid and complex N-linked oligosaccharides (Fig. 2B). N-glycans presenting the LacdiNAc (GalNAc[ $\beta$ →4]GlcNAc) motif were annotated. Three of these structures had the LacdiNAc motif linked to a NeuAc residue in one antenna and presented one, two or three mannose residues in the other. Three other N-glycans presented a fucosylated LacdiNAc motif, similarly to oligosaccharides obtained from the chicken eggshell protein ovocleidin-116 [33]. Like *P. azureus*, the paucimannosidic glycan M<sub>3</sub> was the most abundant structure in the sample, with relative area equivalent to  $15 \pm 7\%$  of all N-glycans ions. Also, core-fucosylated structures, such as F(6)M<sub>2</sub>, were identified (Fig. 1B). Complex N-glycans constituted, jointly, roughly 39% of all glycans found in the skin secretion of *B. raniceps*. Some of the structures annotated in the present work were compatible with N-glycan compositions detected along the embryogenesis of *Xenopus laevis*, and these were identified in Table 1 [34].

### 3.2. O-linked oligosaccharides from *P. azureus* and *B. raniceps* skin secretion

O-linked oligosaccharides were released from glycoproteins in the skin secretion of *P. azureus* and *B. raniceps* by reductive  $\beta$ -elimination, being later purified, derivatized, analyzed by LC-MS/MS, and submitted to automatic annotation and manual verification. Singly and doubly charged sodium adducts ( $[M + Na]^+$  and



**Fig. 1.** LC-MS/MS analysis of N-linked oligosaccharides isolated from amphibian skin secretions. A) Total ion chromatogram (TIC) obtained from permethylated N-glycans isolated from *P. azureus* skin secretion (dotted line) showing the extracted ion chromatogram (XIC), in green, for the ion  $[M + Na]^+ = 1171.5857$  Da. B) Mass spectrum for  $[M + Na]^+ = 1171.5857$  Da. C) Annotated MS/MS spectrum for the precursor ion  $[M + Na]^+ = 1171.5857$  Da with putative structures represented on top of their corresponding ions. D) TIC obtained from permethylated N-glycans isolated from *B. raniceps* skin secretion (dotted line) showing the XIC, in orange, for the ion  $[M + Na]^+ = 1141.5729$  Da. E) Mass spectrum for  $[M + Na]^+ = 1141.5729$  Da. F) Annotated MS/MS spectrum for precursor ion  $[M + Na]^+ = 1141.5729$  Da, compatible with the paucimannosidic structure F(6)M<sub>2</sub>. Legend: ■ N-acetyl glucosamine (GlcNAc), ● Mannose (Man), ▲ Fucose (Fuc).



**Table 1**  
Structures, accurate masses, and charge state of N-linked oligosaccharide identified from skin secretion of *P. azureus* and *B. raniceps* by LC-MS/MS.

Species	Proposed structure, theoretical mass and composition/Oxford nomenclature <sup>a</sup>	$m/z$ <sup>Ex</sup>	$m/z$ <sup>T</sup>	Charge	Error (ppm)	Reference <sup>b</sup>
<i>P. azureus</i>	 m/z: 763.3835 [MONO,perMe,Na,0,freeEnd] Hex1HexNAc2/M1	763.3858	763.3835	1	3.01	
<i>P. azureus/B. raniceps</i>	 m/z: 967.4833 [MONO,perMe,Na,0,freeEnd] Hex2HexNAc2/M2	967.4831	967.4833	1	0.21	G22000 [34]
<i>B. raniceps</i>	 m/z: 1141.5725 [MONO,perMe,Na,0,freeEnd] Hex2HexNAc2Fuc1/F(6)M2	1141.5729	1141.5725	1	0.35	G22100 [34]
<i>P. azureus/B. raniceps</i>	 m/z: 1171.5831 [MONO,perMe,Na,0,freeEnd] Hex3HexNAc2/M3	1171.5857	1171.5831	1	2.22	G23000 [34]
<i>P. azureus</i>	 m/z: 1375.6828 [MONO,perMe,Na,0,freeEnd] Hex4HexNAc2/M4	699.3341	699.336	2	2.72	G24000 [34]
<i>P. azureus/B. raniceps</i>	 m/z: 1579.7826 [MONO,perMe,Na,0,freeEnd] Hex5HexNAc2/M5	801.3869	801.3859	2	1.25	G25000 [34]
<i>P. azureus/B. raniceps</i>	 m/z: 1783.8824 [MONO,perMe,Na,0,freeEnd] Hex6HexNAc2/M6	903.4376	903.4358	2	1.99	G26000 [34]
<i>P. azureus/B. raniceps</i>	 m/z: 1987.9821 [MONO,perMe,Na,0,freeEnd] Hex7HexNAc2/M7	1005.4907	1005.4857	2	4.97	G27000 [34]
<i>B. raniceps</i>	 m/z: 2023.0094 [MONO,perMe,Na,0,freeEnd] Hex3HexNAc4NeuAc1/A1GalNAc1S1	1022.9988	1022.9993	2	0.49	
<i>B. raniceps</i>	 m/z: 2214.1139 [MONO,perMe,Na,0,freeEnd] Hex4HexNAc4Fuc2/F2A2G1	1118.5521	1118.5516	2	0.45	
<i>B. raniceps</i>	 m/z: 2214.1139 [MONO,perMe,Na,0,freeEnd] Hex4HexNAc4Fuc2/F2M4A1GalNAc1	1118.5521	1118.5516	2	0.45	

(continued on next page)

Table 1 (continued)

Species	Proposed structure, theoretical mass and composition/Oxford nomenclature <sup>a</sup>	$m/z$ <sup>Ex</sup>	$m/z$ <sup>T</sup>	Charge	Error (ppm)	Reference <sup>b</sup>
<i>B. raniceps</i>	 m/z: 2227.1091 [MONO,perMe,Na,0,freeEnd] Hex4HexNAc4NeuAc1/M4A1GalNAc1S1	1125.0535	1125.0492	2	3.82	
<i>B. raniceps</i>	 m/z: 2244.1245 [MONO,perMe,Na,0,freeEnd] Hex5HexNAc4Fuc1/M5F1A1GalNAc1	1133.5621	1133.5568	2	4.68	G45100 [34]
<i>B. raniceps</i>	 m/z: 1139.068 [MONO,perMe,Na,0,freeEnd] Hex3HexNAc5Fuc2/F2A2GalNAc1	1139.068	1139.0648	2	2.81	
<i>B. raniceps</i>	 m/z: 2431.2089 [MONO,perMe,Na,0,freeEnd] Hex5HexNAc4NeuAc1/M5A1GalNAc1S1	825.7283	825.7291	3	0.97	G45010 [34]

<sup>Ex</sup> = experimental; <sup>T</sup> = theoretical.

Legend: ■ N-acetyl glucosamine (GlcNAc), ■ N-acetyl galactosamine (GalNAc), ● Mannose (Man), ● Galactose (Gal), ▲ Fucose (Fuc), ◆ Sialic acid (NeuAc).

<sup>a</sup> [MONO, perMe, Na, 0, freeEnd] means [mono charged, permethylated, sodium adducts, non-neutral exchanges, free end structure].

<sup>b</sup> G codes means the glycan compositions from the specific reference, represented by assigning the number of monosaccharides and substituents in order: HexNAc; Hex; Fuc; NeuAc; and phosphate.

[M + 2Na]<sup>2+</sup>) were the predominant ionic species in the samples. The XICs for the ions [M + Na]<sup>+</sup> = 895.4661 Da and 895.4628 Da, found in the *P. azureus* and *B. raniceps* samples, are shown in Fig. 3A and D, respectively, as exemplifications of the O-glycan identification procedures. The corresponding MS and MS/MS spectra are also provided (Fig. 3B–C, E–F). Although the same ion was found in both amphibians, differential product ions (e.g.  $m/z$  298.1612, 620.2866 for *P. azureus* and  $m/z$  284.1463 and 659.3336 for *B. raniceps*) indicate that despite the same glycan composition, HexNAc<sub>1</sub>Hex<sub>1</sub>NeuAc<sub>1</sub>, the sialic acid is differentially connected in the O-glycan isolated for each species (Fig. 3C and F). All annotated MS/MS spectra can be found in Supplementary Material 2, while a list of O-glycan compositions and putative structures, their theoretical, experimental masses and charge states, is available in Table 2.

The XICs for the O-glycans annotated in the skin secretions of both amphibian species were obtained (Fig. 4). The diversity of O-linked glycans from the skin secretion of *B. raniceps* was greater than that of *P. azureus*, which is consistent with what was observed for N-glycans. Some putative O-glycan structures were compatible with those characterized from the egg jelly proteins of other amphibian species, as referenced in Table 2 [6,8,35]. Overall, eight O-glycans were annotated in the *P. azureus* skin extract, while seventeen were found in the corresponding sample from *B. raniceps* (Fig. 4A and B). The skin secretion of *P. azureus* seemed to be constituted mainly by core 1 (or core 8) glycans and derivatives, whereas the skin secretion of *B. raniceps* presented derivatives of the cores 1, 2 and 3, and/or their compositional isomers. Again, O-glycans from *B. raniceps* were structurally more complex than those from *P. azureus*. The HexNAc<sub>1</sub>Hex<sub>1</sub>Fuc<sub>1</sub> glycan (putatively the H Type-3 Antigen) and HexNAc<sub>1</sub>Hex<sub>1</sub>NeuAc<sub>1</sub> (putatively the Sialyl Core 1) were the most abundant O-glycans in *P. azureus* and

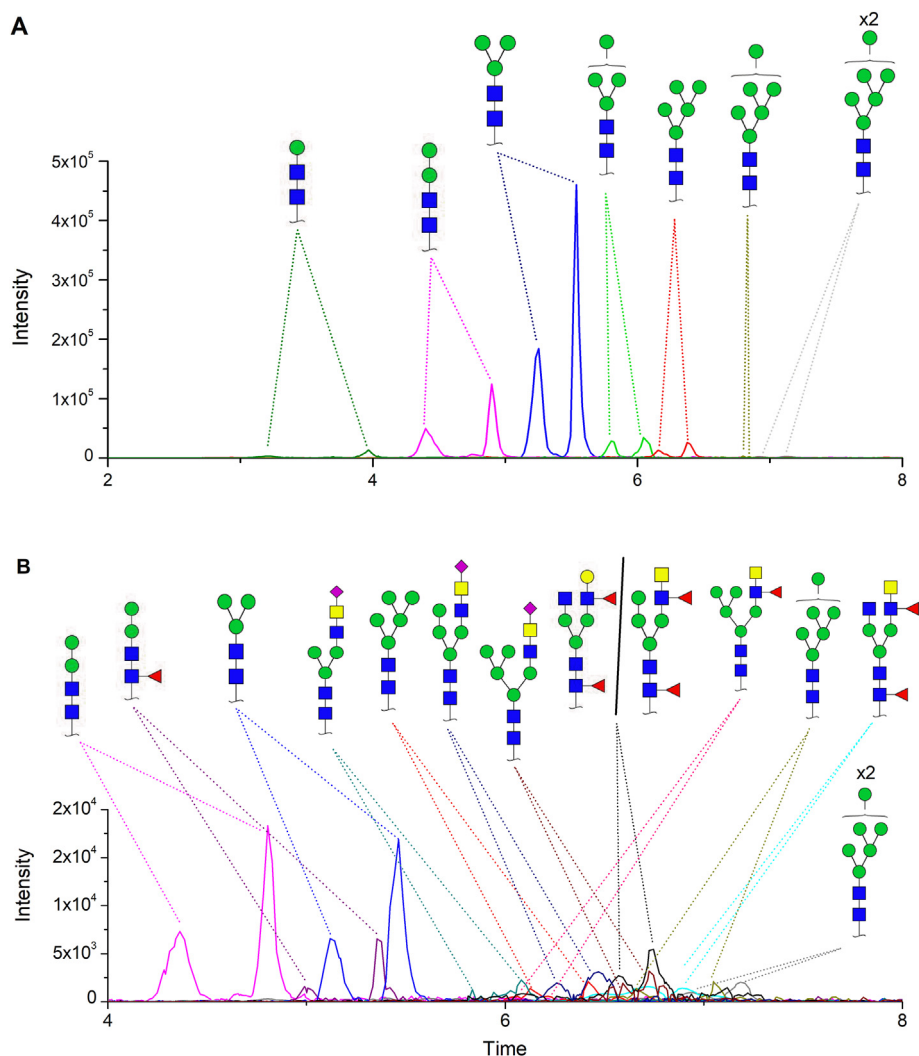
*B. raniceps*, respectively, accounting for nearly 28% and 23% of all O-glycan species identified in these anurans (Supplementary Table 2).

### 3.3. Non-conjugated mono-, di-, tri- and oligosaccharides in the skin secretion of *P. azureus* and *B. raniceps*

To investigate whether non-conjugated mono-, di-, tri- and/or oligosaccharides can be found in the skin secretion of the studied amphibians, a polar fraction of the crude skin extract was obtained and submitted to LC-MS/MS analyses. Again, sodium adducts were the predominant ionic species in MS spectra; however, underivatized monosaccharides produced low intensity ions, and few product ion spectra could be reliably obtained. Nevertheless, ions corresponding to several underivatized glycans species were putatively detected in the MS mode, and their XICs can be found in Fig. 5. Two of these ions produced reliable MS/MS spectra. The ion [M + Na]<sup>+</sup> = 203.0523 Da, compatible with a hexose ([M + Na]<sub>thr</sub><sup>+</sup> = 203.0526, error = 1.5 ppm), was the predominant non-conjugated saccharide detected in the skin secretion of *P. azureus*. Based on the literature, the relative intensities of the ions at  $m/z$  143.0405 and 185.5090 are compatible with mannose, although these are only indicative [36,37]. On the other hand, the ion [M + Na]<sup>+</sup> = 365.1058 Da was the predominant saccharide in the skin secretion of *B. raniceps*, and it was putatively identified as Hex<sub>2</sub> ([M + Na]<sub>thr</sub><sup>+</sup> = 365.1054, error = 1.1 ppm).

### 3.4. Reconstruction of the *P. azureus* and *B. raniceps* N- and O-glycan biosynthesis pathways according to skin tissue transcriptomics data

The dorsal skin tissue of studied amphibians was dissected,



**Fig. 2.** Extracted ion chromatograms (XICs) obtained by LC-MS acquisitions of permethylated N-glycans isolated from A) *P. azureus* and B) *B. raniceps*. Putative structures identified by MS/MS spectra are represented above their corresponding XIC areas. Legend: ■ N-acetyl glucosamine (GlcNAc), ■ N-acetyl galactosamine (GalNAc) ● Mannose (Man), ● Galactose (Gal), ▲ Fucose (Fuc), ◆ Sialic acid (NeuAc).

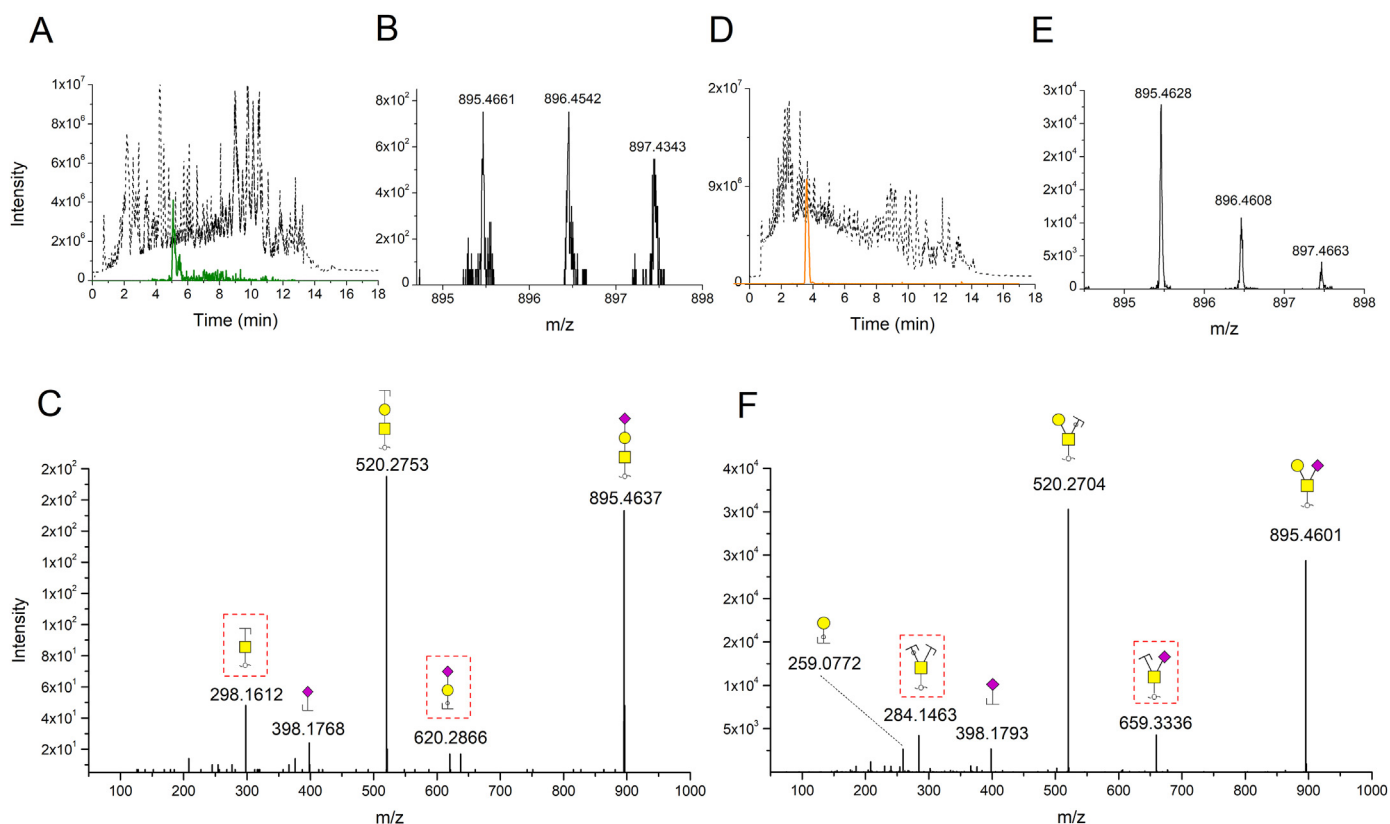
pulverized and submitted to mRNA isolation and 454-sequencing procedures. A total of 664,506 and 627,137 reads with an average length of 376 and 397 bp were obtained for *P. azureus* and *B. raniceps*, respectively. After processing, assemblage of the reading sequences and sequence annotation, transcripts encoding enzymes known to catalyze N- and O-glycan synthesis in vertebrates were investigated and compiled (Tables 3 and 4). All sequences are available at Supplementary Materials 3 (*P. azureus*) and 4 (*B. raniceps*).

The putative N-glycan biosynthesis pathways were reconstructed based on both the glycomics and transcriptomics data (Fig. 6). Overall, there was a conspicuous correlation between glycomics and transcriptomics data, as transcripts for the enzymes necessary for the synthesis of N-glycan structures found in the corresponding amphibians were identified. Although the N-glycans synthesis pathways for *P. azureus* and *B. raniceps* were apparently conserved, as expected, some differences were observed. The precursor encoding the enzyme MAN1A2, responsible for the catalysis of a key step in the synthesis of hybrid and complex N-linked oligosaccharides, was not detected in *P. azureus* transcripts (Fig. 6). This should obstruct the processing of oligomannosidic N-glycan structures in the Golgi apparatus. Similarly, transcripts for *FUT8*, a

gene encoding for an enzyme that catalyzes the fucosylation of the chitobiose core, were not found. This is consistent with the glycomics data, since only non-fucosylated paucimannosidic and mannose rich N-linked oligosaccharides were identified in proteins from the skin secretion of *P. azureus*. Another key observation is that the transcript for the enzyme B4GALNT4, necessary for the synthesis of the LacdiNAc motif, was found exclusively in the *B. raniceps* skin secretion, once again, consistent with the glycomics analyses.

Interestingly, transcripts for the enzyme Beta-hexosaminidase subunit beta (HexB) were abundantly found in the skin secretion of both amphibians. This enzyme is responsible for the synthesis of paucimannosidic glycans in the so-called GnT-I dependent pathway in mammals [38]. This agrees with the presence of paucimannosidic glycans, such as M2F and M3, found in high percentages in the skin secretion of *B. raniceps*. Transcripts for the  $\alpha$ -mannosidase MAN2B2, responsible for the trimming of the M3 paucimannosidic precursor and generation of M2 and M1, were also found in both amphibian species.

Transcripts encoding enzymes in the O-glycan synthesis pathways were also found and used, along with the putative O-glycan structures determined by LC-MS/MS analyses, to model pathways



**Fig. 3.** LC-MS/MS analysis of O-linked oligosaccharides isolated from amphibian skin secretions. A) Total ion chromatogram (TIC) obtained from permethylated O-glycans isolated from *P. azureus* skin secretion (dotted line) showing the extracted ion chromatogram (XIC) (green line) for the ion  $[M + Na]^+ = 895.4661$  Da. B) Mass spectrum for  $[M + Na]^+ = 895.4661$  Da. C) Annotated MS/MS spectrum for the precursor ion  $[M + Na]^+ = 895.4661$  Da with putative structures on top of their corresponding ions, revealing the Sialyl-T antigen. D) TIC obtained from permethylated O-glycans isolated from *B. raniceps* skin secretion (dashed line) showing the XIC (orange line) for the ion  $[M + Na]^+ = 895.4628$  Da. E) Mass spectrum for  $[M + Na]^+ = 895.4628$  Da. F) Annotated MS/MS spectrum for the precursor ion  $[M + Na]^+ = 895.4628$  Da, compatible with the Sialyl Core 1 O-glycan. Red dashed box indicates structures related to daughter ions differentiating Sialyl-T antigen and Sialyl Core 1 O-glycan. Legend: ■ N-acetyl galactosamine (GalNAc), ● Galactose (Gal), ◆ Sialic acid (NeuAc).

in *P. azureus* and *B. raniceps* (Fig. 7). Inherent limitations in glycan structure assignment by mass spectrometry and the higher variability of O-glycan structures makes this a more challenging effort than that for N-glycans, and only glycans whose compositions matched with previously described molecules in egg jelly proteins were considered. However, once more, transcriptomic findings seemed to corroborate with glycomics data. Transcripts encoding GCNT1, ST6GALNAC1-2 and A4GNT were found exclusively in the *B. raniceps* transcriptome, which is consistent with the putative core 2 and 3 structures found for this amphibian in LC-MS/MS analyses (Fig. 7). Furthermore, the transcript encoding the hydroxylase that catalyzes the conversion of cytidine monophosphate (CMP)-NeuAc into CMP-NeuGc was found exclusively in the *B. raniceps* transcriptome, corroborating the structures NeuGc core 1 and NeuGc extended core determined by LC-MS/MS (Table 2).

### 3.5. Prediction of secreted N- and O- glycoproteins in the skin of *P. azureus* and *B. raniceps* from transcriptomic data

To identify putatively secreted glycoproteins in the skin secretion of *P. azureus* and *B. raniceps*, mRNA transcripts were translated *in silico* and submitted to an algorithm for the identification of eukaryotic signal peptide sequences. Subsequently, matching sequences were scanned for potential N- and O-glycosylation sites using NetNGlyc 1.0 and NetOGlyc 4.0. Once identified, these transcripts were submitted to BLAST searches. Transcripts encoding proteins with putative signal peptide sequences, N- and/or O-

glycosylation sequons, and with identity to previously annotated proteins were compiled (Supplementary Materials 5 to 8).

Using this approach, thirty-eight transcripts were identified as putatively secreted glycoproteins containing potential N-glycosylation sites in *P. azureus* (Supplementary Table 3), whereas eighty-four transcripts were identified in *B. raniceps* (Supplementary Table 4). The PANTHER Classification System [31] was used to group predicted N- and O-linked glycoproteins from both amphibians according to their molecular function (Fig. 8). A total of forty-five and twenty-four predicted N-linked glycoproteins from *P. azureus* and *B. raniceps* were respectively ranked in four molecular functions, where glycoproteins with binding functions represented the most abundant class (Fig. 8A): binding (organic cyclic compound binding, heterocyclic compound binding, small molecule binding, carbohydrate derivative binding, ion binding and protein binding), molecular function regulator (transcription regulator activity), catalytic activity (oxidoreductase activity, catalytic activity acting on DNA and hydrolase activity) and transporter activity (transmembrane transporter activity). Several transcripts corresponding to enzymes and enzyme inhibitors were found, indicating that these constitute a significant fraction of the secreted glycoproteins in both amphibians. *P. azureus* and *B. raniceps* presented in common eight transcripts with similarity to N-glycosylated secreted proteins (or their orthologous sequences in different species). These include the enzymes beta-hexosaminidase and dipeptidyl peptidase 1 (cathepsin C), the serine-protease inhibitor ovostatin, and other proteins implicated in cellular adhesion and

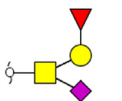
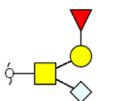
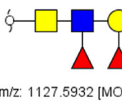

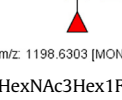
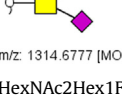
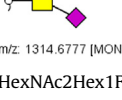
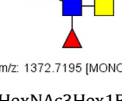


**Table 2**  
Structures, accurate masses, and charge state of O-linked oligosaccharide identified from skin secretion of *P. azureus* and *B. raniceps* by LC-MS.

Species	Proposed structure, theoretical mass and composition/common name <sup>a</sup>	$m/z$ <sup>Ex</sup>	$m/z$ <sup>T</sup>	Charge	Error (ppm)	Reference
<i>P. azureus</i> / <i>B. raniceps</i>	 m/z: 534.2885 [MONO,perMe,Na,0,redEnd]	534.2867	534.2885	1	3.4	FN II-2; VII-6 [7,35]
<i>P. azureus</i> / <i>B. raniceps</i>	HexNAc1Hex1/TF antigen  m/z: 708.3777 [MONO,perMe,Na,0,redEnd]	708.3802	708.3777	1	3.5	FN II-3; VII-6; N-3; 3 and/or 4 [7,9,35,61]
<i>P. azureus</i> / <i>B. raniceps</i>	HexNAc1Hex1Fuc1/H Antigen Type-3  m/z: 738.3883 [MONO,perMe,Na,0,redEnd]	738.3862	738.3883	1	2.8	6 [61]
<i>B. raniceps</i>	HexNAc1Hex2/Extended Core 1 T Antigen  m/z: 779.4148 [MONO,perMe,Na,0,redEnd]	779.4120	779.4148	1	0.3	100-2; N-4 [9,62]
<i>P. azureus</i>	HexNAc2Hex1/Extended Core 1 T Antigen  m/z: 779.4148 [MONO,perMe,Na,0,redEnd]	779.4164	779.4148	1	0.3	VI-3 [35]
<i>P. azureus</i>	HexNAc2Hex1/Extended Core 3  m/z: 895.4621 [MONO,perMe,Na,0,redEnd]	895.4661	895.4621	1	4.5	IV-1 [35]
<i>B. raniceps</i>	HexNAc1Hex1NeuAc1/Sialyl-T Antigen  m/z: 895.4621 [MONO,perMe,Na,0,redEnd]	895.4628	895.4621	1	0.8	IV-3; V-5; 100-6B; 200 II-5 [6,35]
<i>P. azureus</i> / <i>B. raniceps</i>	HexNAc1Hex1NeuAc1/Sialyl Core 1  m/z: 912.4775 [MONO,perMe,Na,0,redEnd]	912.4738	912.4775	1	4.1	C [63]
<i>B. raniceps</i>	HexNAc1Hex2Fuc1/B Antigen Type-3  m/z: 925.4727 [MONO,perMe,Na,0,redEnd]	925.47	925.4727	1	2.9	200-II-5 (22)
<i>B. raniceps</i>	HexNAc1Hex1NeuGc1/NeuGc Core 1  m/z: 953.5040 [MONO,perMe,Na,0,redEnd]	953.5017	953.5040	1	2.4	A7B - HSO <sub>3</sub> (9)
<i>P. azureus</i>	HexNAc2Hex1Fuc1/Fucosylated Core 2  m/z: 983.5146 [MONO,perMe,Na,0,redEnd]	983.5146	983.5151	1	0.5	Extended VI-3 (25)
<i>B. raniceps</i>	HexNAc2Hex2/Extended Core 1 T Antigen  m/z: 1024.5411 [MONO,perMe,Na,0,redEnd]	1024.5453	1024.5411	1	4.1	A7A - HSO <sub>3</sub> (9)
<i>P. azureus</i>	HexNAc3Hex1/Extended Core 2  m/z: 1024.5411 [MONO,perMe,Na,0,redEnd]	1024.5410	1024.5411	1	0.1	Extended VI-3 (25)
	HexNAc3Hex1/Extended Core 1 T Antigen					

(continued on next page)

Table 2 (continued)

Species	Proposed structure, theoretical mass and composition/common name <sup>a</sup>	m/z <sup>Ex</sup>	m/z <sup>T</sup>	Charge	Error (ppm)	Reference
<i>B. raniceps</i>	 m/z: 1069.5514 [MONO,perMe,Na,0,redEnd] HexNAc1Hex1Fuc1NeuAc1/Fucosylated Sialyl Core 1 T Antigen	1069.5540	1069.5514	1	2.4	NFI-11; 100-6A [6]
<i>B. raniceps</i>	 m/z: 1099.5619 [MONO,perMe,Na,0,redEnd] HexNAc1Hex1Fuc1NeuGc1/NeuGc Extended Core 1 T Antigen	1099.5596	1099.5619	1	2.1	Fucosylated 200-II-5 (22)
<i>B. raniceps</i>	 m/z: 1127.5932 [MONO,perMe,Na,0,redEnd] HexNAc2Hex1Fuc2/Extended Core 3	1127.5917	1127.5932	1	1.3	Fucosylated 6 (56)
<i>B. raniceps</i>	 m/z: 1157.6038 [MONO,perMe,Na,0,redEnd] HexNAc2Hex2Fuc1 Extended Core 2	1157.6094	1157.6038	1	4.8	Possibly 9A [64]
<i>B. raniceps</i>	 m/z: 1198.6303 [MONO,perMe,Na,0,redEnd] HexNAc3Hex1Fuc1/Extended Core 2	1198.6293	1198.6303	1	0.8	N-II-8b (8)
<i>B. raniceps</i>	 m/z: 1314.6777 [MONO,perMe,Na,0,redEnd] HexNAc2Hex1Fuc1NeuAc1/Extended Sialyl Core 3	668.8352	668.8335	2	2.5	12A (56)
<i>B. raniceps</i>	 m/z: 1314.6777 [MONO,perMe,Na,0,redEnd] HexNAc2Hex1Fuc1NeuAc1/Extended Sialyl Core 1 T Antigen	668.8352	668.8335	2	2.5	Fucosylated A-12A (9)
<i>B. raniceps</i>	 m/z: 1372.7195 [MONO,perMe,Na,0,redEnd] HexNAc3Hex1Fuc2/Extended Core 2	697.8519	697.8544	2	3.6	NFI-5A (6)

<sup>T</sup> = Theoretical; <sup>Ex</sup> = experimental.

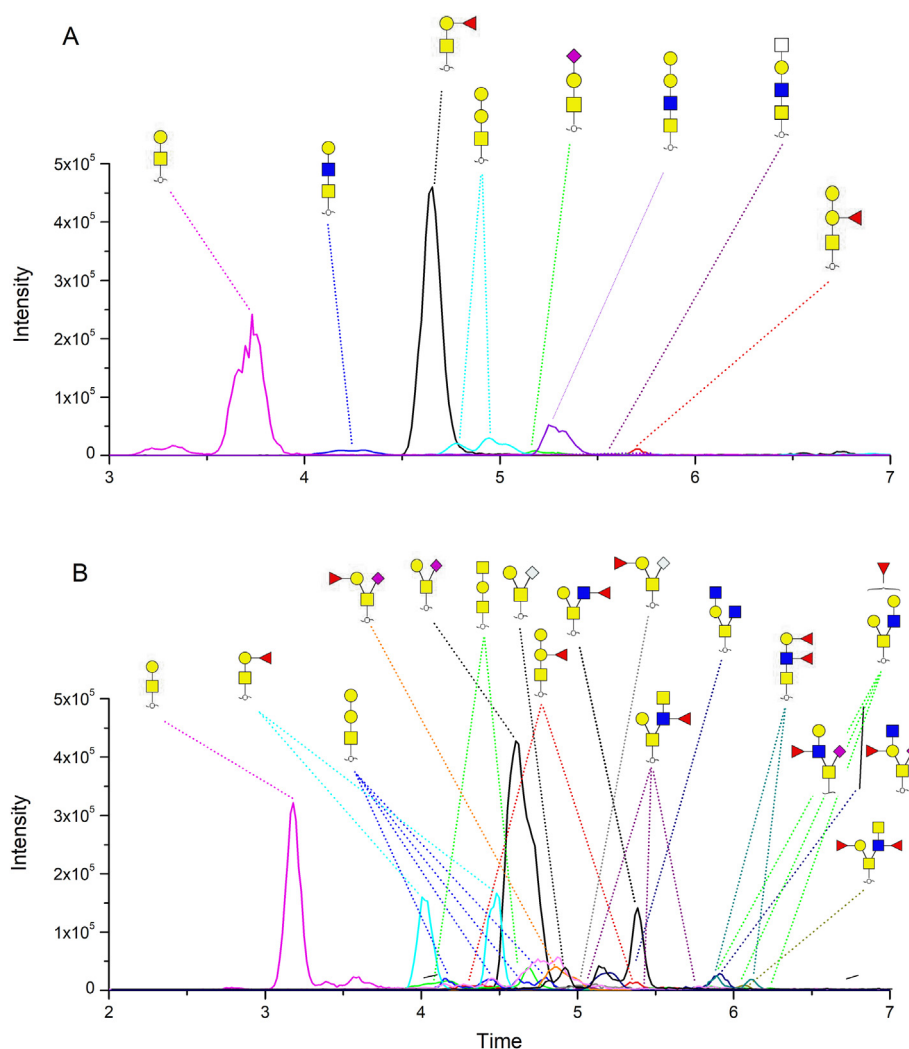
Legend: □ N-acetyl hexosamine (HexNAc), ■ N-acetyl glucosamine (GlcNAc), ◼ N-acetyl galactosamine (GalNAc), ● Mannose (Man), ● Galactose (Gal), ▲ Fucose (Fuc), ◆ Sialic acid (NeuAc), ◆ N-glycolylneuraminic acid (Neu5Gc).

<sup>a</sup> [MONO, perMe, Na, 0, freeEnd] means [mono charged, permethylated, sodium adducts, non-neutral exchanges, reducing-end structure].

cell-cell interactions, such as the CD44 antigen (HCAM - homing cell adhesion molecule) and the SPARC protein (osteonectin). Interestingly, phospholipase A2, previously described in the skin secretion of *P. azureus* [39], and demonstrated by mass spectrometry to contain two N-glycosylation sites occupied by mannose-rich and paucimannose glycans, was also identified in the currently adopted workflow.

In addition, thirty-five transcripts of putatively secreted proteins containing potential O-glycosylation sites were identified in *P. azureus* (Supplementary Table 5), while forty-three transcripts

were identified in *B. raniceps* (Supplementary Table 4). The PANTHER algorithm identified twenty-three and forty-five predicted O-linked glycoproteins from *P. azureus* and *B. raniceps*, respectively (Fig. 8B). Again, most glycoproteins were classified with binding functions. Five transcripts were found in common between the two species, some of them previously identified as also containing potential N-glycosylation sites. Transcripts with identity to the enzyme matrix metalloproteinase-14, involved in the remodeling of the extracellular matrix in humans and other vertebrates [40,41], were identified as putatively secreted O-linked



**Fig. 4.** Extracted ion chromatograms obtained by LC-MS acquisitions of permethylated O-glycans isolated from A) *P. azureus* and B) *B. raniceps*. Putative structures identified by MS/MS spectra are represented above their corresponding XIC areas. Legend: ■ N-acetyl glucosamine (GlcNAc), ■ N-acetyl galactosamine (GalNAc), ● Mannose (Man), ● Galactose (Gal), ▲ Fucose (Fuc), ◆ Sialic acid (NeuAc), ▲ N-glycolylneuraminic acid (Neu5Gc), □ N-acetyl hexosamine (HexNAc).

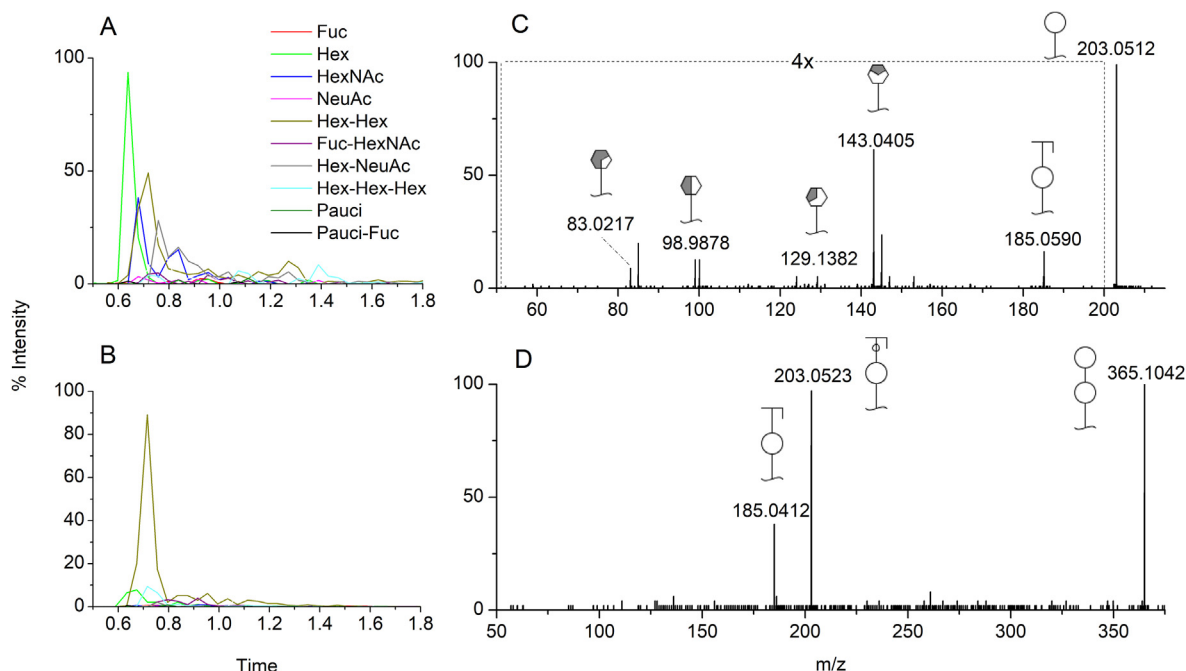
glycoproteins in both amphibians. Interestingly, some transcripts in the skin secretion of *P. azureus* and *B. raniceps* investigated using the present workflow seemed to have non-eukaryotic origin, like a conserved Plasmodium protein of unknown function from *Plasmodium malariae* and an envelope protein of the endogenous *Rhinella marina* retrovirus.

A second analysis was performed to identify whether transcripts encoding proteins that are characteristic of azurophilic granules in neutrophils could be found. In humans, these proteins are the most relevant source of paucimannosidic glycans in infected lung epithelia [32], and therefore, by analogy, constitute probable sources of these molecules in the amphibian epithelia. Indeed, it was found that both amphibians presented transcripts with high identity to the enzymes eosinophil peroxidase and myeloperoxidase (MPO) from other anuran species (Supplementary Material 9). These two enzymes share 68% identity in humans and could not be reliably differentiated in the present analysis. In addition, a transcript with ~75% identity to the CD63 antigen from *Rana temporaria*, also a marker for azurophilic neutrophil granules, was identified in *P. azureus*. These data indicate the presence of transcripts for proteins from azurophilic granules of neutrophils and establish them as a putative source of paucimannosidic glycans.

#### 4. Discussion

The present work presents a first look at the N- and O-linked glycans extracted from glycoconjugates secreted by two amphibian species, their corresponding enzyme synthesis pathways and glycoprotein products, integrating glycomics and transcriptomics data. The annotation of glycan species was performed by mass spectrometry and putative structures were determined by MS/MS fragmentation spectra. It is important to highlight that while other tools, such as nuclear magnetic resonance and high-performance liquid chromatography, might provide more detailed information on the structure of these molecules, mass spectrometry is unrivalled in sensitivity, which is relevant in the present case due to low sample availability.

The most abundant N-glycans in the skin secretion of *P. azureus* and *B. raniceps* were paucimannosidic structures, such as M2, M2F and M3, structures that were previously detected along the early development of *X. laevis* eggs [34]. Paucimannosidic glycans are truncated  $\alpha$ - or  $\beta$ -mannosyl-terminating structures linked to asparagine residues in proteins [38]. These have been widely reported in eukaryotes, like plants, animals, and protists, with the exception of fungi, which produce oligo- and poly- $\alpha$ -mannosylated



**Fig. 5.** Extracted ion chromatograms obtained from LC-MS acquisitions of free saccharides present in the polar fraction of the skin secretion of A) *P. azureus* and B) *B. raniceps* annotated MS/MS spectra of C)  $[M + Na]^+ = 203.0512$  Da and D)  $[M + Na]^+ = 365.1042$  Da corresponding to Hex and Hex<sub>2</sub> structures, respectively. The experiment cannot differentiate hexose isomers (mannose, glucose and galactose).

glycoproteins [38]. Their role in vertebrates is still under debate, as these have been associated with both normal physiological conditions and pathological states [38]. Indeed, in anurans, paucimannosidic glycans might be found in secreted proteins as a consequence of the high rate of cell turnover in the epithelial tissue, similarly to observations regarding the presence of these N-glycan structures in proteins from human buccal epithelial cells (BECs) [42]. In parallel, paucimannosidic glycans might be implicated in the normal or augmented immune response to the ever-present skin commensal and pathogenic bacteria. In humans, it is increasingly clear that the expression of paucimannosidic proteins (glycoproteins containing paucimannosidic glycans) is context-dependent, being linked to processes related to inflammation and infection, cellular differentiation and uncontrolled cell growth [32,38]. It has been demonstrated that proteins in pathogen-infected human lungs contain a high proportion of paucimannosidic glycans as glycoepitopes, while these are negligible in pathogen-free sputum [32]. In amphibians, it is believed that the infiltration of innate immune cells, like neutrophils, corresponds to an early event upon pathogen detection in the anuran skin [43]. Transcripts for neutrophil azurophilic granule protein markers like MPO (or EPX) and CD63 antigen were found in *P. azureus* and/or *B. raniceps* skin extracts, reinforcing that neutrophil proteins might contribute with these structures. However, any parallel between the occurrence and role of paucimannosidic glycans in infected human airways and in anuran skin is, at present, premature. Given that the amphibian skin has a resident commensal microbiota, it is likely that neutrophil products have a role in the maintenance of the tissue homeostasis, acting in consonance with several other mechanisms to control the quality and quantity of the microorganisms over the skin surface, similarly to their role the human gut [44]. Novel experiments aiming to quantify paucimannosidic glycans and canonical inflammatory markers in amphibians challenged with pathogenic bacteria or fungal species, like *Batrachochytrium dendrobatidis*, may shed light on the putative

relation between these glycans species, their harboring proteins, and in the innate immune response of the amphibian skin.

Besides paucimannosidic glycans, M4 and oligomannosidic structures were detected in the *P. azureus* skin secretion, while various hybrid and complex, but less abundant, N-glycans were identified in the *B. raniceps* sample. In *B. raniceps*, N-glycans with LacdiNAc antennae were found. Although the LacdiNAc motif is more commonly encountered in invertebrates, there are numerous reports of their occurrence in vertebrates, including the developmental process of *X. laevis* [34,45]. The higher diversity of N-glycan structures in the skin secretion of *B. raniceps* was accompanied by higher diversity in O-glycan structures for this amphibian. This has prompted us to hypothesize that these observations are a consequence of a higher diversity of secreted glycoproteins in *B. raniceps* skin. According to our predictions of secreted glycoproteins containing N- and O-linked oligosaccharides from the skin transcriptome of both anurans, this is true, a proposition that needs to be further verified experimentally. Indeed, it is important to emphasize that the incompleteness of the signal peptide sequences in some transcripts and incompatibilities regarding as to whether these are targeted for glandular secretion or for skin tissue extracellular matrix, might limit extrapolations concerning the actual presence of these protein products in skin secretions. Therefore, experimental validation of secreted glycoproteins in these anurans is important and should be performed in future studies. Predicted secreted glycoproteins from the skin transcriptome data in *P. azureus* and *B. raniceps* varied, and little overlap between them was observed. This is expected, since the peptide contents of the secretions of these two anurans are largely unrelated [46–49]. Overall, predicted N- and O-glycosylated secreted proteins were mostly serine proteases and serine protease inhibitors, two classes of proteins extensively described in frog skin secretions [50]. Other molecules related to the immune response and reproductive functions, like the immunoglobulin J chain, cathepsin C, and the zona pellucida sperm-binding protein 4-like, were also identified,



**Table 3**  
Annotated enzymes from *P. azureus* and *B. raniceps* transcriptome catalyzing N-glycan synthesis.

Gene	Enzyme description	% Coverage <sup>a</sup>		Length <sup>b</sup>		Nr. reads <sup>c</sup>		Bit Score <sup>d</sup>		Identities (%) <sup>e</sup>		Sequence ID <sup>f</sup>	
		Pa <sup>g</sup>	Br <sup>h</sup>	Pa	Br	Pa	Br	Pa <sup>g</sup>	Br <sup>h</sup>	Pa	Br	Pa	Br
OST	dolichyl-diphosphooligosaccharide-protein glycosyltransferase	65.3	85.2	500	652	70	36	252	841	81	90	XM_030187390.1	XM_040423492.1
MOGS	Mannosyl-oligosaccharide glucosidase	10.0	24.2	240	581	2	5	135	310	77	86	XM_026055988.1	F6U900_XENTR
GANAB	glucosidase II alpha subunit	13.4	61.8	590	2721	8	72	682	3116	88	88	XM_040409011.1	XM_040409011.1
MAN1B1	Endoplasmic reticulum mannosyl-oligosaccharide 1,2-alpha-mannosidase	16.9	8.6	579	294	2	1	257	324	83	87	NM_001093998.1	XM_040405984.1
MAN1A2	mannosyl-oligosaccharide 1,2-alpha-mannosidase	–	12.0	–	362	–	5	–	508	–	92	–	XM_040422787.1
MGAT1	mannosyl (alpha-1,3-)-glycoprotein beta-1,2-N-acetylglucosaminyltransferase	22.7	25.1	449	496	2	7	573	625	90	89	XM_040413474.1	XM_040413474.1
MAN2A2	mannosidase, alpha, class 2A, member 2	11.2	28.6	494	1261	1	18	676	1701	91	91	XM_040414114.1	XM_040414114.1
MGAT2	mannosyl (alpha-1,6-)-glycoprotein beta-1,2-N-acetylglucosaminyltransferase	4.7	13.9	91	272	1	4	135	374	93	92	XM_040411773.1	XM_040411773.1
B4GALT2	Beta-1,4-galactosyltransferase 2	6.2	–	530	–	9	–	440	–	82	–	XR_003858936.1	–
B4GALT3	UDP-Gal:betaGlcNAc beta 1,4- galactosyltransferase 3	37.9	62.6	563	930	2	20	529	887	84	88	XM_040327187.1	XM_040421681.1
B4GALNT4	N-acetyl-beta-glucosaminyl-glycoprotein 4-beta-N-acetylglactosaminyltransferase 1	–	10.8	–	495	–	2	–	660	–	91	–	XM_040410317.1
ST6GALNAC	Alpha-N-acetylglactosaminide alpha-2,6-sialyltransferase	–	6.4	–	153	–	1	–	135	–	83	–	XM_031894018.1
ST6GALNAC2	Alpha-N-acetylglactosaminide alpha-2,6-sialyltransferase 2	–	19.7	–	466	–	2	–	141	–	83	–	XM_031894018.1
ST6GAL1	Beta-galactoside alpha-2,6-sialyltransferase 1	27.8	29.8	541	582	2	7	483	534	85	84	XM_040427853.1	XM_040427853.1
ST3GAL1	CMP-N-acetylneuraminide-beta-galactosamide-alpha-2,3-sialyltransferase 1	16.0	–	474	–	1	–	549	–	88	–	XM_040432183.1	–
ST3GAL2	CMP-N-acetylneuraminide-beta-galactosamide-alpha-2,3-sialyltransferase 2	–	4.2	–	180	–	2	–	289	–	91	–	XP_018112085.1
ST3GAL3	CMP-N-acetylneuraminide-beta-galactosamide-alpha-2,3-sialyltransferase 3	16.0	–	311	–	2	–	235	–	93	–	XM_040407855.1	–
FUT5	4-galactosyl-N-acetylglucosaminide 3-alpha-L-fucosyltransferase	15.1	–	161	–	1	–	176	–	86	–	XM_040408899.1	–
FUT8	alpha (1,6) fucosyltransferase	–	20.7	–	542	–	6	–	571	–	90	–	XM_040411704.1
FUT4	Alpha-(1,3)-fucosyltransferase 4	–	10.5	–	289	–	3	–	228	–	91	–	XM_040426324.1
MGAT4	Alpha-1,3-mannosyl-glycoprotein 4-beta-N-acetylglucosaminyltransferase	21.6	18.3	687	584	3	2	538	852	93	93	XM_040425105.1	XM_040425105.1
HexB	Beta-hexosaminidase subunit beta	67.4	92.0	1418	1936	37	88	1133	1519	81	85	XM_040421446.1	XM_040421446.1
MANBA	Beta-mannosidase	–	3.4	–	687	–	5	–	647	–	88	–	XM_040418222.1
MAN2B2	Alpha-mannosidase	11.9	31.7	350	932	2	5	243	743	90	89	XR_005776409.1	XR_005776409.1

<sup>a</sup> Percentage of coverage obtained for a given sequence encoding an enzyme.

<sup>b</sup> length of the contig obtained (number of nucleotides).

<sup>c</sup> number of the reads in each contig.

<sup>d</sup> score that indicate the statistical significance of the alignment.

<sup>e</sup> percentage of identity of the contig compared to the best matching sequence in database.

<sup>f</sup> identifier of the best sequence matching to the contig.

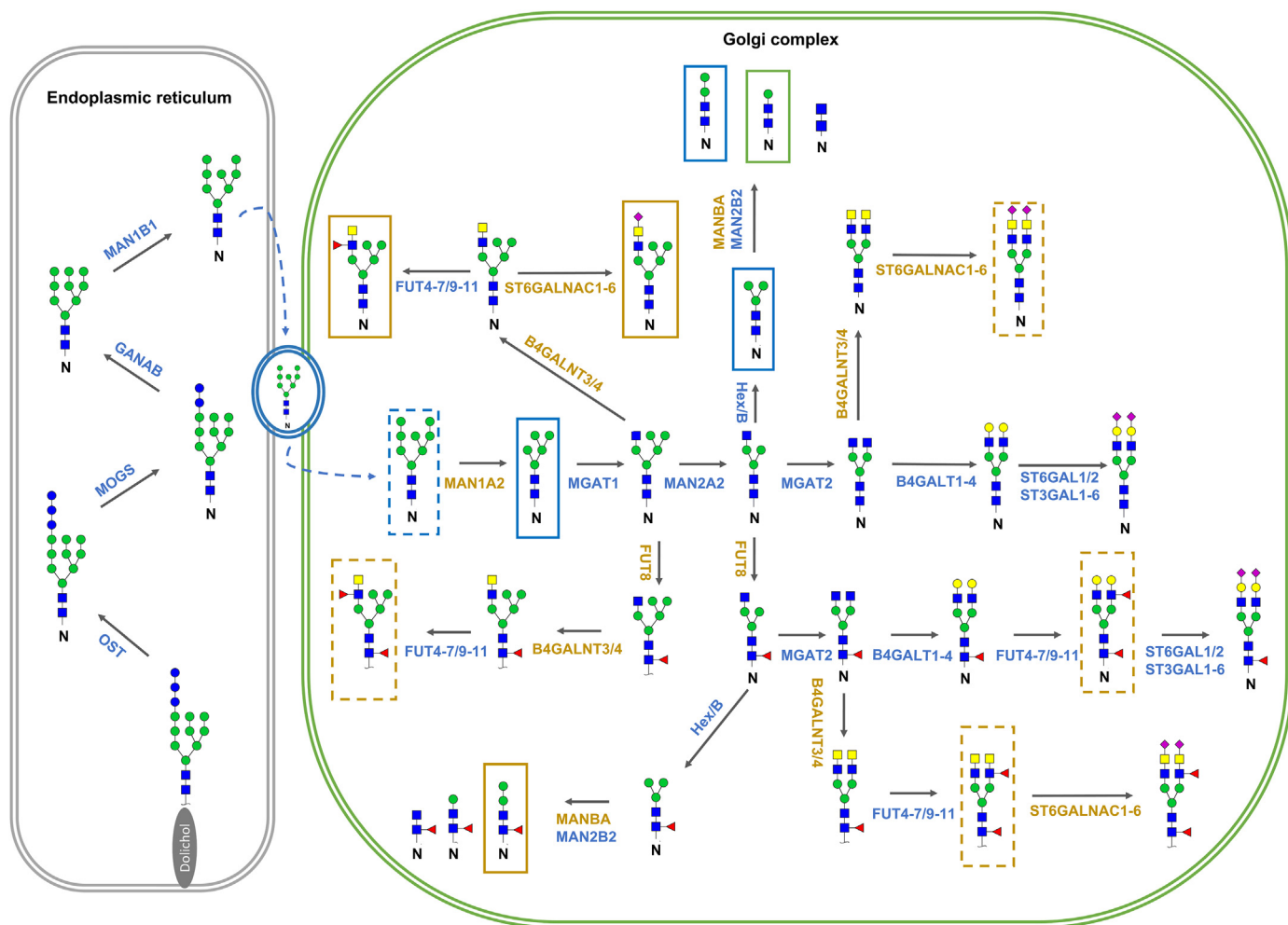
<sup>g</sup> *P. azureus*.

<sup>h</sup> *B. raniceps*.

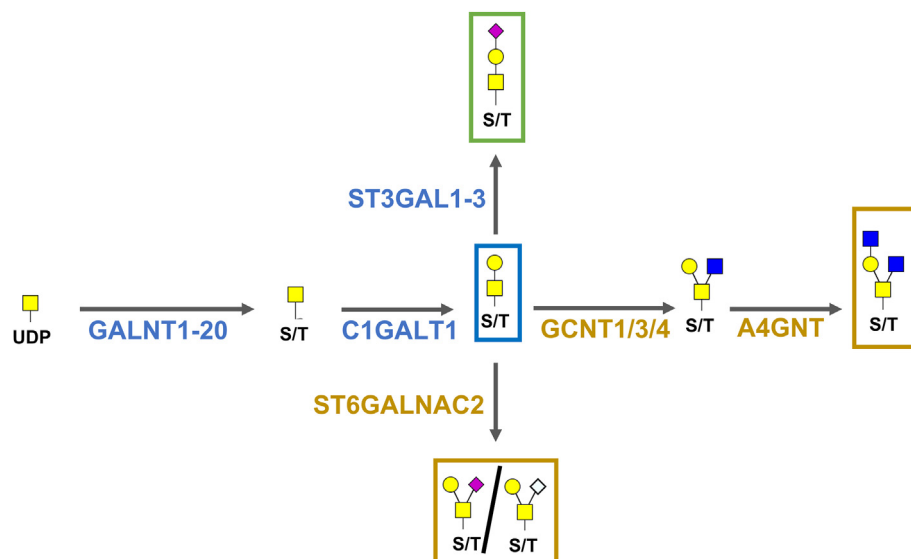
**Table 4**  
Annotated enzymes from *P. azureus* and *B. raniceps* transcriptome catalyzing O-glycan synthesis.

Gene	Enzyme description	% Coverage <sup>a</sup>		Length <sup>b</sup>		Nr. reads <sup>c</sup>		Bit Score <sup>d</sup>		Identities (%) <sup>e</sup>		Sequence ID <sup>f</sup>	
		Pa <sup>g</sup>	Br <sup>h</sup>	Pa	Br	Pa	Br	Pa	Br	Pa	Br	Pa	Br
GALNT6	polypeptide N-acetylgalactosaminyltransferase 4-like	19.7	38.0	410	784	5	9	508	994	89	90	XM_040434107.1	XM_040425911.1
GALNT7	polypeptide N-acetylgalactosaminyltransferase 7	–	12.6	–	660	–	10	–	876	–	91	–	XM_040418669.1
C1GALT1	glycoprotein-N-acetylgalactosamine 3-beta-galactosyltransferase 1-like	47.8	37.2	611	476	9	4	316	603	91	89	XM_040425773.1	XM_040422417.1
B3GNT2	UDP-GlcNAc:betaGal beta-1,3-N-acetylglucosaminyltransferase 2	30.4	–	492	–	6	–	584	–	90	–	XM_040430149.1	–
B3GNT3	UDP-GlcNAc:betaGal beta-1,3-N-acetylglucosaminyltransferase 3	–	48.2	–	905	–	15	–	883	–	84	–	XM_040417462.1
B3GNT7	UDP-GlcNAc:betaGal beta-1,3-N-acetylglucosaminyltransferase 7	–	41.8	–	838	–	13	–	804	–	84	–	XM_040429297.1
GCNT1	beta-1,3-galactosyl-O-glycosyl-glycoprotein beta-1,6-N-acetylglucosaminyltransferase 3-like	–	47.7	–	581	–	8	–	640	–	87	–	XM_040413844.1
B3GALT2	beta-1,3-galactosyltransferase 2	10.9	9.5	457	401	3	5	526	485	73	67	NP_001006126.1	A0A1L8GGL5_XENLA
B3GALT6	Beta-1,3-galactosyltransferase 6	–	6.7	–	170	–	2	–	106	–	85	–	XM_040437146.1
B4GALT2	Beta-1,4-galactosyltransferase 2	6.2	–	530	–	9	–	440	–	82	–	XR_003858936.1	–
B4GALT3	UDP-Gal:betaGlcNAc beta 1,4- galactosyltransferase, polypeptide 3	–	42.1	–	930	–	20	–	887	–	88	–	XM_040421681.1
ST6GALNAC	Alpha-N-acetylgalactosaminide alpha-2,6-sialyltransferase	–	6.4	–	153	–	1	–	135	–	83	–	XM_031894018.1
ST6GALNAC2	Alpha-N-acetylgalactosaminide alpha-2,6-sialyltransferase 2	–	19.6	–	466	–	2	–	141	–	83	–	XM_031894018.1
A4GNT	Alpha-1,4-N-acetylglucosaminyltransferase	–	29.41	–	383	–	20	–	499	–	72	–	A0A2G9RHS2_LITCT
B4GALNT3	N-acetyl-beta-glucosaminyl-glycoprotein 4-beta-N-acetylgalactosaminyltransferase 3	26.3	–	1269	–	5	–	446	–	86	–	XM_040436438.1	–
B4GALNT4	N-acetyl-beta-glucosaminyl-glycoprotein 4-beta-N-acetylgalactosaminyltransferase 4	–	10.8	–	495	–	2	–	660	–	91	–	XM_040410317.1
FUT2	galactoside 2-L-fucosyltransferase	72.1	29.8	1025	424	12	14	1035	219	88	76	XM_040433826.1	XM_040327536.1
FUT4	Alpha-(1,3)-fucosyltransferase 4	–	10.5	–	289	–	3	–	228	–	91	–	XM_040426324.1
FUT5	4-galactosyl-N-acetylglucosaminide 3-alpha-L-fucosyltransferase	15.1	–	161	–	1	–	176	–	86	–	XM_040408899.1	–
POMT1	Protein O-mannosyl-transferase 1	6.9	27.9	173	699	1	5	214	808	79	88	XP_012823681.1	XM_040405143.1
POMGNT1	Protein O-linked-mannose beta-1,2-N-acetylglucosaminyltransferase 1	17.9	55.9	341	1065	2	3	363	479	88	88	XM_040407020.1	XM_040407018.1
ST6GAL1	Beta-galactoside alpha-2,6-sialyltransferase 1	27.7	29.8	541	582	2	7	483	534	85	84	XM_040427853.1	XM_040427853.1
ST3GAL2	CMP-N-acetylneuraminide-beta-galactosamide-alpha-2,3-sialyltransferase 2	–	4.2	–	180	–	2	–	289	–	91	–	NP_001084518.1
ST3GAL3	CMP-N-acetylneuraminide-beta-1,4-galactoside alpha-2,3-sialyltransferase	16.0	–	312	–	2	–	235	–	93	–	XM_040407855.1	–
CMAH	N-acetylneuraminic acid hydroxylase-like	–	17	–	358	–	3	–	363	–	87	–	XM_018556294.1

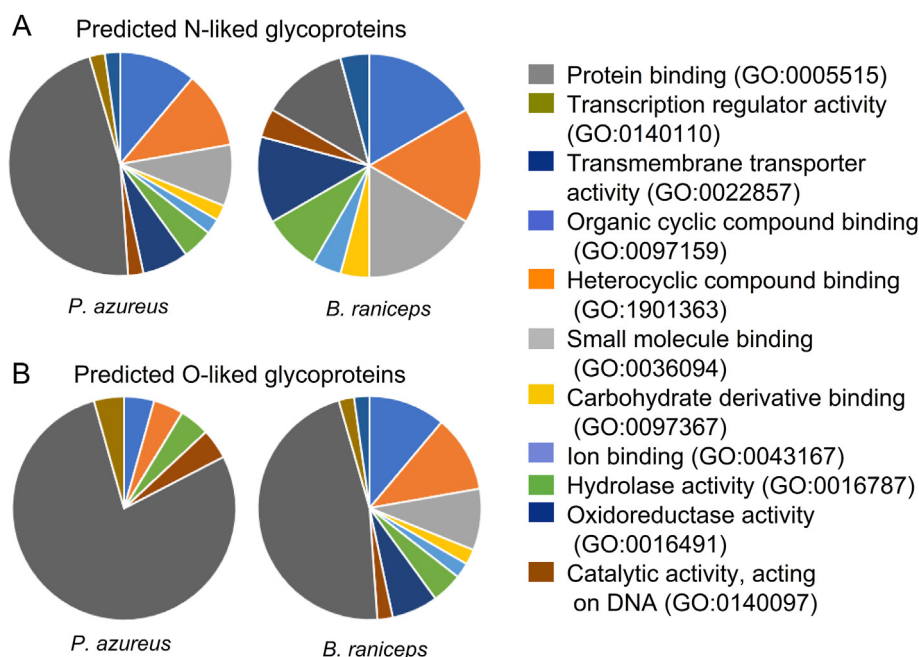
<sup>a</sup> Percentage of coverage obtained for a given sequence encoding an enzyme.<sup>b</sup> length of the contig obtained (number of nucleotides).<sup>c</sup> number of the reads in each contig.<sup>d</sup> score that indicate the statistical significance of the alignment.<sup>e</sup> percentage of identity of the contig compared to the best matching sequence in database.<sup>f</sup> identifier of the best sequence matching to the contig.<sup>g</sup> *P. azureus*.<sup>h</sup> *B. raniceps*.



**Fig. 6.** Putative N-glycosylation biosynthetic pathways for the amphibians *P. azureus* and *B. raniceps* based on the glycomics and transcriptomics data. The genes encoding enzymes are indicated in blue if transcripts were found in both amphibians, green, if transcripts were found exclusively in *P. azureus* skin secretion, and orange if transcripts were found exclusively in *B. raniceps* skin secretion. Squares confining N-glycan structures indicate whether these structures were found in the glycomics investigations. A continuous line square indicates putative N-glycan structures found on the skin secretion of *P. azureus* (green), *B. raniceps* (orange) or both frogs (blue). Dotted line squares indicate N-glycan structures that were not found on skin secretions but may have been partially hydrolysed for the generation of “trimmed N-glycans”, these detected in LC-MS/MS experiments. The same color pattern introduced above is used. Legend: ■ N-acetyl glucosamine (GlcNAc), ■ N-acetyl galactosamine (GalNAc), ● Glucose (Glc), ● Mannose (Man), ● Galactose (Gal), ▲ Fucose (Fuc), ◆ Sialic acid (NeuAc).



**Fig. 7.** Putative mucin glycosylation pathways based on the glycomics and transcriptomics data for the amphibians *P. azureus* and *B. raniceps*. The genes encoding enzymes are indicated as their occurrence in skin secretion of *B. raniceps* (orange) or both amphibians (blue). Boxes over O-glycan structures indicate whether these were identified in the LC-MS/MS glycomics studies. A continuous line box indicates putative O-glycan structures found in the skin secretion. Legend: ■ N-acetyl glucosamine (GlcNAc), ■ N-acetyl galactosamine (GalNAc), ● Galactose (Gal), ◆ Sialic acid (NeuAc), ◆ N-glycolylneuraminic acid (Neu5Gc).



**Fig. 8.** Gene ontology molecular function of predicted A) N- and B) O-linked glycoproteins from the *P. azureus* and *B. raniceps* transcriptome, respectively. Note that subfamilies of molecular function were used.

as well as proteins that interact with extracellular matrix components, such as dystroglycan and the matrix metalloproteinase 2. Interestingly,  $\beta$ -hexosaminidase, a protein associated with the generation of paucimannosidic glycans in nematodes, plants and insects [51], was discovered in the transcriptome analyses of both anurans. It is difficult to establish biological roles for glycans in such a vast array of proteins with varied biological functions. Indeed, they might be related to a wide spectrum of biological activities depending on their housing proteins, such as structural effects, as well as involvement in intrinsic and extrinsic recognition events [52].

One interesting question is whether the hydrolysis of mature glycan species contributes to the diversity of N- and O-glycans found in proteins from the skin secretion of the studied anurans. Although the meaning of these findings remain uncertain, non-conjugated saccharides were found in the skin extract of *P. azureus* and *B. raniceps*, and transcripts from bacterial, fungal, protozoal, and viral sources were putatively annotated serendipitously in their skin transcriptomes. This suggests that endo- and exo-glycosidases of bacterial and protozoal origins are candidates in the hydrolysis of complex glycan structures [53]. Mucin glycan-metabolizing gene clusters are abundant in prevalent



commensals and rare in pathogens in the human gut [54] and it is thus possible that protein-linked glycans have a similar role in the amphibian skin, favoring the commensal microorganisms over the pathogenic. In addition, lysosomal glycosidases, which would be responsible for endogenous glycan hydrolysis, were not found despite extensive searches in the skin transcriptome of both anurans. Further experiments need to be performed to verify whether glycosidase activity can be found in the skin secretion of amphibians and to determine possible bacterial and/or protozoal origin.

The putative biosynthetic pathways of N- and O-linked oligosaccharides in the skin of *P. azureus* and *B. raniceps* were consistent with those determined for other chordates [55]. The most distinctive feature between the N-glycan synthesis pathway of these two amphibians is that no transcripts for the enzyme MAN1A2 were found in the skin of *P. azureus*. This indicates that the M8 (Man<sub>8</sub>) glycan arising from the endoplasmic reticulum cannot be processed any further in the Golgi complex, making unfeasible the synthesis of complex structures in the skin, an observation confirmed by glycomics data. The primary consequence of this finding is that paucimannosidic glycans cannot be generated via the GnT-I dependent pathway, indicating that an independent route or even alternative pathways are the most probable sources for these N-glycans in the skin secretion of *P. azureus* [38]. A different scenario is observed for *B. raniceps*. This amphibian is capable of synthesizing GlcNAc<sub>3</sub>Man<sub>5</sub>, enabling the GnT-I truncation pathway as well as the GnT-I independent pathway for the synthesis of paucimannosidic structures. The expression of the enzymes GnT-I and GnT-II in the skin tissue of *X. laevis* was previously demonstrated [56,57], suggesting that the lack of such transcripts in *P. azureus* warrants further investigation. O-glycosylation pathways were also partially distinct between studied amphibians since some transcripts were only found in *B. raniceps*. For example, transcripts for ST6GALNAC and ST6GALNAC2 were found exclusively in the *B. raniceps* skin. Although genomic data need to be acquired to verify the absence of these genes, it is not unprecedented that related organisms harbor differences in the protein-linked glycan content. *P. azureus* is from the Phyllomedusidae family while *B. raniceps* is from the Hylidae family, and therefore, these clades have been probably evolving independently since the Paleogene period [58]. Particularities in their niches, especially in the interactions these amphibians undertake with microorganisms, such as bacteria, viruses, fungi and protozoa, are likely candidates for the observed differences in N- and O-glycan contents between *P. azureus* and *B. raniceps*. Indeed, the evasion of infectious agents is considered the most probable evolutionary force for humans not expressing N-glycolylneuraminic acid (Neu5Gc), while other non-hominid primates and mammals do [59]. Novel studies on the protein-linked glycans of other anurans will provide further data on the overall diversity of glycans in amphibian skin secretions in relation to their phylogeny and provide more clues to their putative relations with the microbiota within their niches.

## 5. Conclusion

The present work reports the N- and O-glycan products and associated pathways in the skin secretion of *P. azureus* and *B. raniceps*. Also, it describes putatively N- and O-glycosylated protein products in the secretion of these anurans. Although a large amount of data is presented, this is an exploratory work; therefore, further investigations will be necessary to reveal the actual ecological and evolutionary roles performed by N- and O-linked oligosaccharides in the skin secretion of amphibians. Experiments aiming to evaluate changes in the abundance and diversity of protein-linked oligosaccharides in the amphibian skin secretions in response to an external stimulus (like microorganisms) should

serve as a first approach. Finally, the results presented herein corroborate previous studies that suggest that the amphibian skin is a model for the study of the human gut and its interaction with the resident microbiota [15]. N- and O- protein linked glycans and their putative degradation by enzymes produced by the resident microbiota might constitute yet another level of similarity between these two systems, and their description might be invaluable as a model for the understanding of the tripartite relationships between host, microbiome, and pathogens [60] that are commonly observed in nature.

## Funding

This study was supported by the Coordenação de Aperfeiçoamento de Pessoal de Nível Superior - Brasil (CAPES) - Finance Code 001. This work was also supported by: Fundação de amparo a pesquisa do DF (FAP-DF, [www.fap.df.gov.br](http://www.fap.df.gov.br)) grant 00193.0000145/2019–72.

## Author contributions

EAB – conceptualization, investigation and Writing – original draft; GSCA – investigation, formal analysis; MMAC – investigation; HLS – investigation; FSR – investigation; JBN – investigation; MSW – investigation; ACA – resources; GDB – conceptualization and Writing – original draft.

## Declaration of interests

The authors declare no competing interests.

## Acknowledgements

We would like to dedicate this work in the loving memory of Filipe Souza da Rocha, a young chemist with a bright future that left us too early. We would also like to thank Daniel C. Moreira for the critical reading of the manuscript, EMBRAPA Genetic Resources and Biotechnology, especially Dr. Carlos Bloch Júnior, and the Institute of Chemistry of University of Brasília for the laboratory support.

## Appendix A. Supplementary data

Supplementary data to this article can be found online at <https://doi.org/10.1016/j.biochi.2022.01.008>.

## References

- [1] V. Mutt, An appreciation of the work of Vittorio Ersamer, *Peptides* 2 (1981) 3–6, [https://doi.org/10.1016/0196-9781\(81\)90002-4](https://doi.org/10.1016/0196-9781(81)90002-4).
- [2] L.H. Lazarus, M. Attila, The toad, ugly and venomous, wears yet a precious jewel in his skin, *Prog. Neurobiol.* 41 (1993) 473–507, [https://doi.org/10.1016/0301-0082\(93\)90027-P](https://doi.org/10.1016/0301-0082(93)90027-P).
- [3] E. König, O.R.P. Bininda-Emonds, C. Shaw, The diversity and evolution of anuran skin peptides, *Peptides* 63 (2015) 96–117, <https://doi.org/10.1016/j.peptides.2014.11.003>.
- [4] J.W. Daly, C.W. Myers, N. Whittaker, Further classification of skin alkaloids from neotropical poison frogs (dendrobatidae), with a general survey of toxic/noxious substances in the amphibia, *Toxicon* 25 (1987) 1023–1095, [https://doi.org/10.1016/0041-0101\(87\)90265-0](https://doi.org/10.1016/0041-0101(87)90265-0).
- [5] V. Ersamer, P. Melchiorri, Active polypeptides of the amphibian skin and their synthetic analogues, *Pure Appl. Chem.* 35 (1973) 463–494, <https://doi.org/10.1351/pac197335040463>.
- [6] A. Coppin, E. Maes, G. Strecker, Species-specificity of amphibia carbohydrate chains: the *Bufo viridis* case study, *Carbohydr. Res.* 337 (2002) 121–132, [https://doi.org/10.1016/S0008-6215\(01\)00301-9](https://doi.org/10.1016/S0008-6215(01)00301-9).
- [7] A. Coppin, E. Maes, C. Flahaut, B. Coddeville, G. Strecker, Acquisition of species-specific O-linked carbohydrate chains from oviducal mucins in *Rana arvalis*. A case study, *Eur. J. Biochem.* 266 (1999) 370–382, <https://doi.org/10.1046/j.1432-1327.1999.00862.x>.
- [8] R. Mourad, W. Morelle, A. Neveu, G. Strecker, Diversity of O-linked

- glycosylation patterns between species. Characterization of 25 carbohydrate chains from oviductal mucins of *Rana ridibunda*, *Eur. J. Biochem.* 268 (2001) 1990–2003, <https://doi.org/10.1046/j.1432-1327.2001.02071.x>.
- [9] D. Florea, E. Maes, M. Haddad, G. Strecker, Structural analysis of the oligosaccharide alditols released from the jelly coat of *Rana dalmatina* eggs by reductive  $\beta$ -elimination, *Biochimie* 84 (2002) 611–624, [https://doi.org/10.1016/S0300-9084\(02\)01432-3](https://doi.org/10.1016/S0300-9084(02)01432-3).
- [10] E. Dubaissi, K. Rousseau, G.W. Hughes, C. Ridley, R.K. Grecnis, I.S. Roberts, D.J. Thornton, Functional characterization of the mucus barrier on the Xenopus tropicalis skin surface, *Proc. Natl. Acad. Sci. Unit. States Am.* 115 (2018) 726, <https://doi.org/10.1073/pnas.1713539115>, LP – 731.
- [11] J. Lombard, The multiple evolutionary origins of the eukaryotic N-glycosylation pathway, *Biol. Direct* 11 (2016) 36, <https://doi.org/10.1186/s13062-016-0137-2>.
- [12] A. Varki, R.D. Cummings, J.D. Esko, H.H. Freeze, P. Stanley, C.R. Bertozzi, G.W. Hart, M.E. Etzler, *Essentials of Glycobiology*, Cold Spring Harbor Laboratory Press, 2009.
- [13] A.P. Corfield, M. Berry, Glycan variation and evolution in the eukaryotes, *Trends Biochem. Sci.* 40 (2015) 351–359, <https://doi.org/10.1016/j.tibs.2015.04.004>.
- [14] B. Schiller, A. Hykollari, S. Yan, K. Paschinger, I.B.H. Wilson, Complicated N-linked glycans in simple organisms, *Biol. Chem.* 393 (2012) 661–673, <https://doi.org/10.1515/hsz-2012-0150>.
- [15] B.M. Colombo, T. Scalvenzi, S. Benlamara, N. Pollet, Microbiota and mucosal immunity in amphibians, *Front. Immunol.* 6 (2015) 111, <https://doi.org/10.3389/fimmu.2015.00111>.
- [16] J.B. Walke, M.H. Becker, S.C. Loftus, L.L. House, G. Cormier, R. V. Jensen, L.K. Belden, Amphibian skin may select for rare environmental microbes, *ISME J.* 8 (2014) 2207–2217, <https://doi.org/10.1038/ismej.2014.77>.
- [17] V.J. McKenzie, R.M. Bowers, N. Fierer, R. Knight, C.L. Lauber, Co-habiting amphibian species harbor unique skin bacterial communities in wild populations, *ISME J.* 6 (2012) 588–596, <https://doi.org/10.1038/ismej.2011.129>.
- [18] R.N. Harris, R.M. Brucker, J.B. Walke, M.H. Becker, C.R. Schwantes, D.C. Flaherty, B. a Lam, D.C. Woodhams, C.J. Briggs, V.T. Vredenburg, K.P.C. Minbiole, Skin microbes on frogs prevent morbidity and mortality caused by a lethal skin fungus, *ISME J.* 3 (2009) 818–824, <https://doi.org/10.1038/ismej.2009.27>.
- [19] N.M. Koropatkin, E.A. Cameron, E.C. Martens, How glycan metabolism shapes the human gut microbiota, *Nat. Rev. Microbiol.* 10 (2012) 323–335, <https://doi.org/10.1038/nrmicro2746>.
- [20] R.L. Cramp, R.K. McPhee, E.A. Meyer, M.E. Ohmer, C.E. Franklin, First line of defence: the role of sloughing in the regulation of cutaneous microbes in frogs, *Conserv. Physiol.* 2 (2014), <https://doi.org/10.1093/conphys/cou012> cou012.
- [21] J.F.A. Varga, M.P. Bui-Marinis, B.A. Katzenback, Frog skin innate immune defences: sensing and surviving pathogens, *Front. Immunol.* 9 (2019) 3128, <https://doi.org/10.3389/fimmu.2018.03128>.
- [22] W. Morelle, J.-C. Michalski, Analysis of protein glycosylation by mass spectrometry, *Nat. Protoc.* 2 (2007) 1585–1602, <https://doi.org/10.1038/nprot.2007.227>.
- [23] D. Kolarich, E. Rapp, W.B. Struwe, S.M. Haslam, J. Zaia, R. McBride, S. Agravat, M.P. Campbell, M. Kato, R. Ranzinger, C. Kettner, W.S. York, The minimum information required for a glycomics experiment (MIRAGE) project: improving the standards for reporting mass-spectrometry-based glyco-analytic data, *Mol. Cell. Proteomics* 12 (2013) 991–995, <https://doi.org/10.1074/mcp.O112.026492>.
- [24] Y. Watanabe, K.F. Aoki-Kinoshita, Y. Ishihama, S. Okuda, GlycoPOST realizes FAIR principles for glycomics mass spectrometry data, *Nucleic Acids Res.* 49 (2021), <https://doi.org/10.1093/NAR/GKAA1012>, D1523–D1528.
- [25] A. Varki, R.D. Cummings, M. Aebi, N.H. Packer, P.H. Seeberger, J.D. Esko, P. Stanley, G. Hart, A. Darvill, T. Kinoshita, J.J. Prestegard, R.L. Schnaar, H.H. Freeze, J.D. Marth, C.R. Bertozzi, M.E. Etzler, M. Frank, J.F. Vliegenthart, T. Lütteke, S. Perez, E. Bolton, P. Rudd, J. Paulson, M. Kanehisa, P. Toukach, K.F. Aoki-Kinoshita, A. Dell, H. Narimatsu, W. York, N. Taniguchi, S. Kornfeld, Symbol nomenclature for graphical representations of glycans, *Glycobiology* 25 (2015) 1323–1324, <https://doi.org/10.1093/glycob/cwv091>.
- [26] A. Sebben, *Fisiologica a Fresco : Uma Nova Visao Sobre a Anatomia De Anfíbios E Repteis*, Herpetol. Do Bras. II., 1986.
- [27] B. Chevreur, T. Pfisterer, B. Drescher, A.J. Driesel, W.E.G. Müller, T. Wetter, S. Suhai, Using the miraEST assembler for reliable and automated mRNA transcript assembly and SNP detection in sequenced ESTs, *Genome Res.* 14 (2004) 1147–1159, <https://doi.org/10.1101/gr.1917404>.
- [28] H. Nielsen, Predicting secretory proteins with SignalP, *Methods Mol. Biol.* 1611 (2017) 59–73, [https://doi.org/10.1007/978-1-4939-7015-5\\_6](https://doi.org/10.1007/978-1-4939-7015-5_6).
- [29] R. Gupta, S. Brunak, Prediction of glycosylation across the human proteome and the correlation to protein function, *Pac. Symp. Biocomput.* (2002) 310–322.
- [30] C. Steentoft, S.Y. Vakhrushev, H.J. Joshi, Y. Kong, M.B. Vester-Christensen, K.T.-B.G. Schjoldager, K. Lavrsen, S. Dabelsteen, N.B. Pedersen, L. Marcos-Silva, R. Gupta, E.P. Bennett, U. Mandel, S. Brunak, H.H. Wandall, S.B. Levery, H. Clausen, Precision mapping of the human O-GalNAc glycoproteome through SimpleCell technology, *EMBO J.* 32 (2013) 1478–1488, <https://doi.org/10.1038/emboj.2013.79>.
- [31] H. Mi, D. Ebert, A. Muruganujan, C. Mills, L.-P. Albu, T. Mushayama, P.D. Thomas, PANTHER version 16: a revised family classification, tree-based classification tool, enhancer regions and extensive API, *Nucleic Acids Res.* 49 (2021) D394–D403, <https://doi.org/10.1093/NAR/GKAA1106>.
- [32] M. Thaysen-Andersen, V. Venkatakrishnan, I. Loke, C. Laurini, S. Diestel, B.L. Parker, N.H. Packer, Human neutrophils secrete bioactive paucimannosidic proteins from azurophilic granules into pathogen-infected sputum, *J. Biol. Chem.* 290 (2015) 8789–8802, <https://doi.org/10.1074/jbc.M114.631622>.
- [33] M. Nimitz, H.S. Conrad, K. Mann, LacidiNac (GalNAc $\beta$ 1-4GlcNAc) is a major motif in N-glycan structures of the chicken eggshell protein ovocleidin-116, *Biochim. Biophys. Acta* 1675 (2004) 71–80, <https://doi.org/10.1016/j.bbagen.2004.08.007>.
- [34] Y. Qu, K.M. Dubiak, E.H. Peuchen, M.M. Champion, Z. Zhang, A.S. Hebert, S. Wright, J.J. Coon, P.W. Huber, N.J. Dovichi, Quantitative capillary zone electrophoresis-mass spectrometry reveals the N-glycome developmental plan during vertebrate embryogenesis, *Mol. Omi.* 16 (2020) 210–220, <https://doi.org/10.1039/D0MO00005A>.
- [35] D. Florea, E. Maes, Y. Guérardel, A. Page, J.-P. Zanetta, D. Cogalniceanu, G. Strecker, Structure elucidation of NeuAc, NeuGc and Kdn-containing O-glycans released from *Triturus alpestris* oviductal mucins. Characterization of the poly LacdiNac sequence: HSO3(4)(GalNAc $\beta$ 1-4GlcNAc $\beta$ 1-3)1-3GalNAc $\beta$ 1-4(GlcNAc $\beta$ 1-3)0-1GlcNAc $\beta$ 1-6GalNAc, *Glycoconj. J.* 23 (2006) 377–399, <https://doi.org/10.1007/s10719-006-6126-4>.
- [36] Z. Zhu, L. Song, J.E. Bartmess, Differentiation of underivatized monosaccharides by atmospheric pressure chemical ionization quadrupole time-of-flight mass spectrometry, *Rapid Commun. Mass Spectrom.* 26 (2012) 1320–1328, <https://doi.org/10.1002/rcm.6229>.
- [37] X. Zhu, T. Sato, The distinction of underivatized monosaccharides using electrospray ionization ion trap mass spectrometry, *Rapid Commun. Mass Spectrom.* 21 (2007) 191–198, <https://doi.org/10.1002/rcm.2825>.
- [38] H.C. Tjondro, I. Loke, S. Chatterjee, M. Thaysen-Andersen, Human protein paucimannosylation: cues from the eukaryotic kingdoms, *Biol. Rev.* 94 (2019) 2068–2100, <https://doi.org/10.1111/brv.12548>.
- [39] B.B.P. Souza, J.L. Cardozo Fh, A.M. Murad, M.V. Prates, M.M.A. Coura, G.D. Brand, E.A. Barbosa, C. Bloch, Identification and characterization of phospholipases A<sub>2</sub> from the skin secretion of *Pithecopus azureus* anuran, *Toxicol* 167 (2019), <https://doi.org/10.1016/j.toxicon.2019.06.002>.
- [40] W. Lin, M. Bonin, A. Boden, R. Wieduwild, P. Murawala, M. Wermke, H. Andrade, M. Bornhäuser, Y. Zhang, Peptidyl prolyl cis/trans isomerase activity on the cell surface correlates with extracellular matrix development, *Commun. Biol.* 2 (2019) 58, <https://doi.org/10.1038/s42003-019-0315-8>.
- [41] S.H. Taylor, C.Y.C. Yeung, N.S. Kalsom, Y. Lu, P. Zigrino, T. Starborg, S. Warwood, D.F. Holmes, E.G. Canty-Laird, C. Mauch, K.E. Kadler, Matrix metalloproteinase 14 is required for fibrous tissue expansion, *Elife* 4 (2015), <https://doi.org/10.7554/eLife.09345>.
- [42] A. V. Everest-Dass, D. Jin, M. Thaysen-Andersen, H. Nevalainen, D. Kolarich, N.H. Packer, Comparative structural analysis of the glycosylation of salivary and buccal cell proteins: innate protection against infection by *Candida albicans*, *Glycobiology* 22 (2012) 1465–1479, <https://doi.org/10.1093/glycob/cws112>.
- [43] L.F. Grogan, J. Robert, L. Berger, L.F. Skerratt, B.C. Scheele, J.G. Castley, D.A. Newell, H.I. McCallum, Review of the Amphibian immune response to chytridiomycosis, and future directions, *Front. Immunol.* 9 (2018) 2536, <https://doi.org/10.3389/fimmu.2018.02536>.
- [44] D. Zhang, P.S. Frenette, Cross talk between neutrophils and the microbiota, *Blood* 133 (2019) 2168–2177, <https://doi.org/10.1182/blood-2018-11-844555>.
- [45] D.H. Van den Eijnden, A.P. Neeleman, W.P. Van der Knaap, H. Bakker, M. Agterberg, I. Van Die, Novel glycosylation routes for glycoproteins: the lacidiNac pathway, *Biochem. Soc. Trans.* 23 (1995) 175–179, <https://doi.org/10.1042/bst0230175>.
- [46] B.S. Magalhães, J.A.T. Melo, J.R.S.A. Leite, L.P. Silva, M. V. Prates, F. Vinecky, E.A. Barbosa, R.M. Verly, A. Mehta, J.R. Nicoli, M.P. Bemquerer, A.C. Andrade, C.J. Bloch, Post-secretory events alter the peptide content of the skin secretion of *Hypsiboas raniceps*, *Biochem. Biophys. Res. Commun.* 377 (2008) 1057–1061, <https://doi.org/10.1016/j.bbrc.2008.10.102>.
- [47] C.S.F.C. Popov, B.S. Magalhães, B.J. Goodfellow, A.L. Bocca, D.M. Pereira, P.B. Andrade, P. Valentão, P.J.B. Pereira, J.E. Rodrigues, P.H. de Holanda Veloso, T.M.B. Rezende, Host-defense peptides AC12, DK16 and RC11 with immunomodulatory activity isolated from *Hypsiboas raniceps* skin secretion, *Peptides* 113 (2019) 11–21, <https://doi.org/10.1016/j.peptides.2018.12.007>.
- [48] G.D. Brand, J.R.S.A. Leite, S.M. de Sá Mandel, D.A. Mesquita, L.P. Silva, M.V. Prates, E.A. Barbosa, F. Vinecky, G.R. Martins, J.H. Galasso, S.A.S. Kuckelhaus, R.N.R. Sampaio, J.R. Furtado, A.C. Andrade, C. Bloch, Novel dermaseptins from *Phyllomedusa hypochondrialis* (Amphibia), *Biochem. Biophys. Res. Commun.* 347 (2006) 739–746, <https://doi.org/10.1016/j.bbrc.2006.06.168>.
- [49] G.D. Brand, F.C. Krause, L.P. Silva, J.R.S.A. Leite, J.A.T. Melo, M.V. Prates, J.B. Pesquero, E.L. Santos, C.R. Nakaie, C.M. Costa-Neto, C. Bloch, Bradykinin-related peptides from *Phyllomedusa hypochondrialis*, *Peptides* 27 (2006) 2137–2146, <https://doi.org/10.1016/j.peptides.2006.04.020>.
- [50] J.M. Conlon, J.B. Kim, A protease inhibitor of the Kunitz family from skin secretions of the tomato frog, *dyscophus guineti* (microhylidae), *Biochem. Biophys. Res. Commun.* 279 (2000) 961–964, <https://doi.org/10.1006/bbrc.2000.4052>.
- [51] M. Gutternigg, D. Kretschmer-Lubich, K. Paschinger, D. Rendić, J. Hader, P. Geier, R. Ranftl, V. Jantsch, G. Lochnit, I.B.H. Wilson, Biosynthesis of

- truncated N-linked oligosaccharides results from non-orthologous hexosaminidase-mediated mechanisms in nematodes, plants, and insects, *J. Biol. Chem.* 282 (2007) 27825–27840, <https://doi.org/10.1074/jbc.M704235200>.
- [52] A. Varki, Biological roles of glycans, *Glycobiology* 27 (2017) 3–49, <https://doi.org/10.1093/glycob/cwv086>.
- [53] J. Garbe, M. Collin, Bacterial hydrolysis of host glycoproteins - powerful protein modification and efficient nutrient acquisition, *J. Innate Immun.* 4 (2012) 121–131, <https://doi.org/10.1159/000334775>.
- [54] K.M. Pruss, A. Marcobal, A.M. Southwick, D. Dahan, S.A. Smits, J.A. Ferreyra, S.K. Higginbottom, E.D. Sonnenburg, P.C. Kashyap, B. Choudhury, L. Bode, J.L. Sonnenburg, Mucin-derived O-glycans supplemented to diet mitigate diverse microbiota perturbations, *ISME J.* 15 (2021) 577–591, <https://doi.org/10.1038/s41396-020-00798-6>.
- [55] K.T. Schjoldager, Y. Narimatsu, H.J. Joshi, H. Clausen, Global view of human protein glycosylation pathways and functions, *Nat. Rev. Mol. Cell Biol.* 21 (2020) 729–749, <https://doi.org/10.1038/s41580-020-00294-x>.
- [56] J. Mucha, B. Svoboda, S. Kappel, R. Strasser, P. Bencur, U. Fröhwein, H. Schachter, L. Mach, J. Glössl, Two closely related forms of UDP-GlcNAc: alpha6-D-mannoside beta1,2-N-acetylglucosaminyltransferase II occur in the clawed frog *Xenopus laevis*, *Glycoconj. J.* 19 (2002) 187–195, <https://doi.org/10.1023/A:1024201824354>.
- [57] J. Mucha, B. Svoboda, U. Fröhwein, R. Strasser, M. Mischinger, H. Schwihla, F. Altmann, W. Hane, H. Schachter, J. Glössl, L. Mach, Tissues of the clawed frog *Xenopus laevis* contain two closely related forms of UDP-GlcNAc:alpha3-D-mannoside beta-1,2-N-acetylglucosaminyltransferase I, *Glycobiology* 11 (2001) 769–778, <https://doi.org/10.1093/glycob/11.9.769>.
- [58] Y.-J. Feng, D.C. Blackburn, D. Liang, D.M. Hillis, D.B. Wake, D.C. Cannatella, P. Zhang, Phylogenomics reveals rapid, simultaneous diversification of three major clades of Gondwanan frogs at the Cretaceous–Paleogene boundary, *Proc. Natl. Acad. Sci. Unit. States Am.* 114 (2017) E5864–E5870, <https://doi.org/10.1073/pnas.1704632114>.
- [59] M.O. Altman, P. Gagneux, Absence of Neu5Gc and presence of anti-Neu5Gc antibodies in humans—an evolutionary perspective, *Front. Immunol.* 10 (2019) 789, <https://doi.org/10.3389/fimmu.2019.00789>.
- [60] X.A. Harrison, S.J. Price, K. Hopkins, W.T.M. Leung, C. Sergeant, T.W.J. Garner, Diversity–stability dynamics of the Amphibian skin microbiome and susceptibility to a lethal viral pathogen, *Front. Microbiol.* 10 (2019) 2883, <https://doi.org/10.3389/fmicb.2019.02883>.
- [61] A. Coppin, E. Maes, W. Morelle, G. Strecker, Structural analysis of 13 neutral oligosaccharide-alditols released by reductive beta-elimination from oviducal mucins of *Rana temporaria*, *Eur. J. Biochem.* 266 (1999) 94–104, <https://doi.org/10.1046/j.1432-1327.1999.00823.x>.
- [62] W. Morelle, G. Strecker, Isolation of the O-glycosidically linked oligosaccharides obtained by alkaline borohydride degradation from oviducal mucins of the toad *Bufo bufo*, *J. Chromatogr. B Biomed. Sci. Appl.* 706 (1998) 101–111, [https://doi.org/10.1016/s0378-4347\(97\)00442-8](https://doi.org/10.1016/s0378-4347(97)00442-8).
- [63] Y. Guéardel, O. Kol, E. Maes, T. Lefebvre, B. Boilly, M. Davril, G. Strecker, O-glycan variability of egg-jelly mucins from *Xenopus laevis*: characterization of four phenotypes that differ by the terminal glycosylation of their mucins, *Biochem. J.* 352 Pt 2 (2000) 449–463.
- [64] Y. Guéardel, D. Petit, T. Madigou, B. Guillet, E. Maes, A. Maftah, D. Boujard, G. Strecker, O. Kol, Identification of the blood group Lewis(a) determinant in the oviducal mucins of *Xenopus tropicalis*, *FEBS Lett.* 554 (2003) 330–336, [https://doi.org/10.1016/s0014-5793\(03\)01183-9](https://doi.org/10.1016/s0014-5793(03)01183-9).